Monograph:
Tokhi, M.O., Kourtis, S., Poerwanto, H. et al. (1 more author) (1995) Open-Loop Control of Flexible Manipulator Systems Using Filtered Inputs. Research Report. ACSE Research Report 598 . Department of Automatic Control and Systems Engineering

---

Department
AUTOMAT
CONTR
and SYSTE
ENGINEERING
UNIVERSITY of SHEFFIELD

OPEN-LOOP CONTROL OF FLEXIBLE MANIPULATOR SYSTEMS USING FILTERED INPUTS

M O Tokhi, S Kourtis, H Poerwanto, and A K M Azad

Department of Automatic Control and Systems Engineering,
The University of Sheffield, Mappin Street, Sheffield, S1 3JD, UK.

Tel: + 44 (0)114 282 5136.
Fax: + 44 (0)114 273 1729.
E-mail: O.Tokhi@sheffield.ac.uk.

Research Report No. 598

August 1995

Abstract

This paper presents an investigation into the development of open-loop control strategies for flexible manipulator systems using filtering techniques. Shaped torque inputs, including lowpass and bandstop filtered torque input functions, are developed and used in an open-loop configuration and their performances within a simulation environment characterising a constrained planar single-link flexible manipulator system studied in comparison to a bang-bang torque input. Simulation results verifying the performance of the developed control strategies are presented and discussed.

Key words: *Butterworth filter, distributed parameter systems, elliptic filter, filtered torque input, flexible manipulators, open-loop control.*

CONTENTS

LIST OF TABLES AND FIGURES

1 Introduction

Open-loop control methods for vibration suppression in flexible manipulator systems consist of developing the control input through a consideration of the physical and vibrational properties of the system. The method involves development of suitable forcing functions so that to reduce the vibrations at resonance modes. The methods commonly developed include shaped command methods, computed torque technique and bang-bang control. The shaped command methods attempt to develop forcing functions that minimise residual motion (vibration) and the effect of parameters that affect the resonance modes (Aspinwall, 1980; Meckl and Seering, 1985a,b, 1987, 1988, 1990; Singer and Seering, 1988, 1990, 1992, Swigert, 1980; Wang, 1986). Common problems of concern encountered in these methods include long move (response) time, instability due to un-reduced modes and controller robustness in case of large change of the manipulator dynamics.

In the computed torque approach, depending on the detailed model of the system and desired output trajectory, the torque input is calculated using a model inversion process (Alberts et.al, 1990; Bayo, 1988; Moulin and Bayo, 1991). The technique suffers from several problems, due to, for instance, model inaccuracy, uncertainty over implementability of the desired trajectory, sensitivity to system parameter variation and response time penalties for a causal input.

Bang-bang control involves the utilisation of single and multiple switch bang-bang control functions (Dellman et.al, 1956; Onsay and Akay, 1991). Bang-bang control functions require accurate selection of switching time, depending on the representative dynamic model of the system. Minor modelling error could cause switching error and, thus, result in a substantial increase in the residual vibrations (Sangveraphunsiri, 1984). Although, utilisation of minimum energy inputs has been shown to eliminate the problem of switching times that arise in the bang-bang input (Jayasuriya and Choupra, 1991), the total response time, however, becomes longer (Meckl and Seering, 1990; Onsay and Akay, 1991).

The aim of this investigation is to develop control methods to reduce motion induced vibration in flexible manipulator systems during fast movements. The assumption is that the motion itself is the main source of system vibration. Thus, torque profiles which do not contain energy at system natural frequencies do not excite structural vibration and hence require no additional settling time. The procedure for determining shaped inputs that generate fast motions with minimum residual vibration has previously been addressed (Bayo, 1988; Meckl and Seering, 1988). The torque input needed to move the flexible manipulator from one point to another without vibration must have several properties: *(a)* it should have an acceleration and deceleration phase, *(b)* it should be able to be scaled for different step motions, and *(c)* it should have as sharp a cutoff frequency as required. These three properties of the required torque input will allow driving the manipulator system as quickly as possible without exciting its resonance modes.

Open-loop shaped torque inputs are developed in this paper on the basis of extracting the energies around the natural frequencies using filter theory so that the vibration in the flexible manipulator system is reduced during and after the movement. Not much work has been done on the extraction of energy at the system resonance modes using filters. The filters are used here for pre-processing the input to the plant, so that no energy is ever put into the system near its resonance modes.

2 The flexible manipulator system environment

The single-link flexible manipulator considered in this paper is described in Figure 1, where, I_h represents the hub inertia of the manipulator. A payload mass M_p with its associated inertia I_p is attached to the end-point. A control torque $\tau(t)$ is applied at the hub by an actuator motor. The angular displacement of the manipulator, in moving in the $POQ-$plane, is denoted by $\theta(t)$. The manipulator is assumed to be stiff in vertical bending and torsion, thus, allowing it to vibrate (be flexible) dominantly in the horizontal direction. The shear deformation and rotary inertia effects are also ignored.

For an angular displacement θ and an elastic deflection u the total (net) displacement $y(x,t)$ of a point along the manipulator at a distance x from the hub can be described as a function of both the rigid body motion $\theta(t)$ and elastic deflection $u(x,t)$ measured from the line OX;

$$y(x,t) = x\theta(t) + u(x,t) \tag{1}$$

Thus, it follows from equation (1) that in such a system, the control action is to take account of both the rigid body motion and the elastic motion (vibration).

The dynamic equations of motion of the manipulator can be obtained using the Hamilton's extended principle (Meirovitch, 1967) with the associated kinetic, potential and dissipated energies of the system. Ignoring the effects of the rotary inertia and shear deformation the governing equation of motion of the manipulator incorporating a mode frequency dependent damping term can be obtained as (Tokhi et.al, 1995)

$$EI\frac{\partial^4 y(x,t)}{\partial x^4} + \rho\frac{\partial^2 y(x,t)}{\partial t^2} - D_s\frac{\partial^3 y(x,t)}{\partial x^2 \partial t} = \tau(t) \tag{2}$$

with the corresponding boundary and initial conditions as

$$\begin{aligned} &y(0,t) = 0 && , \quad I_h\frac{\partial^3 y(0,t)}{\partial x \partial t^2} - EI\frac{\partial^2 y(0,t)}{\partial x^2} = \tau(t) \\ &M_p\frac{\partial^2 y(l,t)}{\partial t^2} - EI\frac{\partial^3 y(l,t)}{\partial x^3} = 0 && , \quad EI\frac{\partial^2 y(l,t)}{\partial x^2} = 0 \\ &y(x,0) = 0 && , \quad \frac{\partial y(x,0)}{\partial x} = 0 \end{aligned} \tag{3}$$

where D_s, I, ρ and E represent the resistance to strain velocity, area moment of inertia, mass density per unit length of the manipulator and Young modulus respectively. Equation (2) gives the fourth-order partial differential equation (PDE) which represents the dynamic equation describing the motion of the flexible manipulator. To solve this equation and thus, develop a suitable simulation environment characterising the behaviour of the system, the finite difference (FD) method can be used. Thus, a set of equivalent difference equations defined by the central finite difference quotients of the FD method are obtained by discretising the PDE in equation (2) with its associated boundary and initial conditions in

equation (3). The process involves dividing the manipulator into n sections each of length Δx and considering the deflection of each section at sample times Δt. In this manner, a solution of the PDE is obtained by generating the central difference formulae for the partial derivative terms of the response $y(x,t)$ of the manipulator at points $x = i\Delta x$, $t = j\Delta t$ (Tokhi et.al, 1995);

$$\mathbf{Y}_{i,j+1} = \mathbf{A}\mathbf{Y}_{i,j} + \mathbf{B}\mathbf{Y}_{i,j-1} + \mathbf{C}\mathbf{F} \tag{4}$$

where $\mathbf{Y}_{i,j+1}$ is the displacement of grid points $i = 1,2,\cdots,n$ of the manipulator at time step $j+1$, $\mathbf{Y}_{i,j}$ and $\mathbf{Y}_{i,j-1}$ are the corresponding displacements at time step j and $j-1$ respectively. $\mathbf{A}$ and $\mathbf{B}$ are constant $n \times n$ matrices whose entries depend on the flexible manipulator specification and the number of sections the manipulator is divided into, $\mathbf{C}$ is a constant matrix related to the given input torque and $\mathbf{F}$ is an $n \times 1$ matrix related to the time step Δt and mass per unit length of the manipulator;

$$\mathbf{Y}_{i,j+1} = \begin{bmatrix} y_{1,j+1} \\ y_{2,j+1} \\ \vdots \\ y_{n,j+1} \end{bmatrix}, \quad \mathbf{Y}_{i,j} = \begin{bmatrix} y_{1,j} \\ y_{2,j} \\ \vdots \\ y_{n,j} \end{bmatrix}, \quad \mathbf{Y}_{i,j-1} = \begin{bmatrix} y_{1,j-1} \\ y_{2,j-1} \\ \vdots \\ y_{n,j-1} \end{bmatrix}$$

$$\mathbf{A} = \begin{bmatrix} K_1 & K_2 & K_3 & 0 & 0 & \cdots & 0 & 0 \\ (b+d) & (a-2d) & (b+d) & -c & 0 & \cdots & 0 & 0 \\ -c & (b+d) & (a-2d) & (b+d) & -c & \cdots & 0 & 0 \\ \vdots & \ddots & \ddots & \ddots & \ddots & \ddots & \ddots & \vdots \\ 0 & 0 & \cdots & -c & b+d & a-2d & b+d & -c \\ 0 & 0 & \cdots & 0 & K_7 & K_8 & K_9 & K_{10} \\ 0 & 0 & \cdots & 0 & 0 & K_{14} & K_{15} & K_{16} \end{bmatrix}$$

$$\mathbf{B} = \begin{bmatrix} K_4 & K_5 & 0 & 0 & 0 & \cdots & 0 & 0 \\ -d & 2d-1 & -d & 0 & 0 & \cdots & 0 & 0 \\ 0 & -d & 2d-1 & -d & 0 & \cdots & 0 & 0 \\ \vdots & \ddots & \ddots & \ddots & \ddots & \ddots & \ddots & \vdots \\ 0 & 0 & \cdots & 0 & -d & 2d-1 & -d & 0 \\ 0 & 0 & \cdots & 0 & 0 & K_{11} & K_{12} & K_{13} \\ 0 & 0 & \cdots & 0 & 0 & 0 & 0 & K_{17} \end{bmatrix}$$

$$\mathbf{C} = \tau(j) \quad , \mathbf{F} = \begin{bmatrix} K_6 & 0 & \cdots & 0 \end{bmatrix}^T$$

where, $a = 2 - \frac{6EI\Delta t^2}{\rho\Delta x^4}$, $b = \frac{4EI\Delta t^2}{\rho\Delta x^4}$, $c = \frac{EI\Delta t^2}{\rho\Delta x^4}$, $d = \frac{D_S\Delta t}{\rho\Delta x^2}$ and

$$K_1 = \frac{c\Delta t^2 EI + 2c\Delta x I_h + (a-2d)\Delta t^2 EI}{\Delta t^2 EI + c\Delta x I_h}, \quad K_2 = \frac{(b+d)\Delta t^2 EI}{\Delta t^2 EI + c\Delta x I_h},$$

$$K_3 = -\frac{c\Delta t^2 EI}{\Delta t^2 EI + c\Delta x I_h}, \quad K_4 = -\frac{c\Delta x I_h + (1-2d)\Delta t^2 EI}{\Delta t^2 EI + c\Delta x I_h},$$

$$K_5 = -\frac{d\Delta t^2 EI}{\Delta t^2 EI + c\Delta x I_h}, \quad K_6 = \frac{c\Delta x^2{}_\Delta t^2}{\Delta t^2 EI + c\Delta x I_h},$$

$$K_7 = -c, \quad K_8 = (b+d), \quad K_9 = (a+c-2d),$$

$$K_{10} = -(2c-b-d), \quad K_{11} = -d, \quad K_{12} = -(1-2d), \quad K_{13} = -d,$$

$$K_{14} = \frac{-2c\Delta t^2 EI}{\Delta t^2 EI + 2c\Delta x^3 M_P}, \quad K_{15} = \frac{4c\Delta t^2 EI}{\Delta t^2 EI + 2c\Delta x^3 M_P},$$

$$K_{16} = \frac{\Delta t^2 EI}{\Delta t^2\, EI + 2c\Delta x^3 M_P}\left\{a + 2b - 4c + \frac{4c\Delta x^3 M_P}{\Delta t^2 EI}\right\},$$

$$K_{17} = \frac{-\Delta t^2 EI}{\Delta t^2\, EI + 2c\Delta x^3 M_P}\left\{\frac{2c\Delta x^3 M_P}{\Delta t^2 EI} + 1\right\}.$$

Equation (4) is the required relation for the simulation of the flexible manipulator that can be implemented on a digital processor easily.

3 Filtered torque input

The filtered torque input strategy adopted here is to use a single cycle of a square wave, which is known to give optimal response, and filter out any spectral energy near the natural frequencies. The filters thus designed are for pre-processing the input to the plant so that no energy is ever put into the system near its resonance modes. Note that real-time processing requirement is imposed. The simplest method to remove energy at system natural frequencies is to pass the square wave through a lowpass filter. This will attenuate all frequencies above the filter cutoff frequency. The most important consideration is to achieve a steep roll-off rate at the cutoff frequency so that energy can be passed for frequencies nearly up to the lowest natural frequency of the flexible manipulator. An alternative method to remove energy at system natural frequencies will be to use

(narrowband) bandstop filters with centre frequenceis at selected (dominant) resonance modes of the system.

There are various types of filter, namely, Butterworth, Chebyshev and elliptic, which can be employed. Here Butterworth and elliptic filters are used. These filters have the desired frequency response in magnitude, allow for any desired cutoff rate and are physically realisable. The magnitude of the frequency response of a lowpass Butterworth filter is given by (Jackson, 1989)

$$|H(j\omega)|^2 = \frac{1}{1+\left(\frac{\omega}{\omega_c}\right)^{2n}} = \frac{1}{1+\varepsilon\left(\frac{\omega}{\omega_p}\right)^{2n}} \tag{5}$$

where, n is a positive integer signifying the order of the filter, ω_c is the filter cutoff frequency (−3 dB frequency), ω_p is the passband edge frequency and $\left(1+\varepsilon^2\right)^{-1}$ is the band edge value of $|H(j\omega)|^2$. Note that $|H(j\omega)|^2$ is monatomic in both the passband and stopband. The order of the filter required to yield an attenuation δ_2 at a specified frequency ω_s (stopband edge frequency) is easily determined from equation (5) as

$$n = \frac{\log\left\{\frac{1}{\delta_2^2}-1\right\}}{2\log\left\{\frac{\omega_s}{\omega_c}\right\}} = \frac{\log\left\{\frac{\delta_1}{\varepsilon}\right\}}{\log\left\{\frac{\omega_s}{\omega_p}\right\}} \tag{6}$$

where, by definition, $\delta_2 = \left(1+\delta_1^2\right)^{-0.5}$. Thus, the Butterworth filter is completely characterised by the parameters n, δ_2, ε and the ratio $\frac{\omega_s}{\omega_p}$.

Equation (6) can be employed with arbitrary δ_1, δ_2, ω_c and ω_s to yield the required filter order n, from which the filter design is readily obtained. The Butterworth approximation results from the requirement that the magnitude response be maximally flat in both the passband and the stopband. That is, the first $(2n-1)$ derivatives of $|H(j\omega)|^2$ are specified to be equal to zero at $\omega = 0$ and at $\omega = \infty$.

The sharpest transition from passband to stopband for given filter specifications is achieved by an elliptic filter design. Thus, the elliptic design is optimum in this sense. The

magnitude response of an elliptic filter is equi-ripple in both the passband and stopband. The squared magnitude response of a lowpass elliptic filter is of the form (Zverev, 1967)

$$|H(j\omega)|^2 = \frac{1}{1+\eta^2 U_n^2\left\{\frac{\omega}{\omega_c}\right\}}$$

where $U_n\{\omega\}$ is a Jacobian elliptic function of order n and η is a parameter related to the passband ripple. It is known that most efficient designs occur when the approximation error is equally spread over the passband and stopband. Elliptic filters allow this objective to be achieved easily, thus, being most efficient from the viewpoint of yielding the smallest-order filter for a given set of specifications. Equivalently, for a given order and a given set of specifications, an elliptic filter has the smallest transition bandwidth.

The filter order required for a passband ripple γ_1, stopband ripple γ_2, and transition ratio $\frac{\omega_p}{\omega_s}$ is given as

$$n = \frac{K\left\{\frac{\omega_s}{\omega_c}\right\}K\left\{\left(1-\frac{\eta^2}{\gamma_1^2}\right)^{0.5}\right\}}{K\left\{\frac{\eta}{\gamma_1}\right\}K\left\{\left(1-\frac{\omega_p^2}{\omega_s^2}\right)^{0.5}\right\}}$$

where $K\{v\}$ is the complete elliptic integral of the first kind, defined as

$$K\{v\} = \int_0^{\pi/2}\left(1-v^2\sin^2\varphi\right)^{-0.5}d\varphi$$

$\gamma_2 = \left(1+\gamma_1^{\,2}\right)^{-0.5}$ and $\gamma_1 = 10\log\left(1+\eta^2\right)$. Values of the above integral are given in tabulated from in a number of text books (Dwight, 1957). The phase response of an elliptic filter is more nonlinear in the passband than a comparable Butterworth filter, especially near the band edge.

The design relations for the lowpass filters given above can be utilised in normalised form to design the corresponding bandstop filters. This involves a transformation from lowpass to bandstop filter (Banks, 1990).

4 Simulation results

In the simulation results presented an aluminium type single-link flexible manipulator of parameters and characteristics given in Table 1 is considered. To investigate the performance of the control strategies, an FD simulation environment of the manipulator was developed by dividing the manipulator into 19 sections. The algorithm was implemented, with $D_s = 0$, within the Simulink environment (The Mathworks, 1992). To verify the control strategies with the filtered torque inputs, the performance of the system is studied in comparison to a bang-bang torque input for a similar input level in each case. In general, the system dynamics are dominantly characterised by the first two flexible modes. Thus, from a practical viewpoint, the system vibrations can be reduced to an acceptable level by concentrating the control effort to the first two flexible modes of the system. In this investigation, however, the measurement/performance range is confined to $0-100$ Hz, coverering the first three resonance modes of the system.

4.1 Bang-bang torque input

The system was first excited with the bang-bang toque input shown in Figure 2 and its response was monitored at the hub and end-point. Figure 3 shows the hub displacement. It is noted that the system response is oscillatory throughout the measurement period. The first three resonance modes of the system are located at 12.07 Hz, 38.1 Hz and 74 Hz respectively. These are reasonably close to those of the actual system, thus, verifying the performance of the simulation algorithm in characterising the behaviour of the flexible manipulator. The oscillatory nature of the system response and accuracy of the simulation algorithm is further evidenced in the hub velocity, end-point acceleration and end-point residual motion (vibration) of the system, as shown in Figure 4. The end-point residual motion is obtained by using a high-pass filter to extract the flexible motion from the system response at the end-point. Although, the accuracy of the simulation environment can further be enhanced by dividing the manipulator into a larger number of sections within the FD discretisation process, for purposes of this investigation, the level of accuracy achieved

with 19 sections is reasonably acceptable. Note further that increasing the number of sections leads to an increase in the computational burden on the digital processor and thus slows the computational process. It is noted, that the system response with the bang-bang torque input has reached a desired steady-state level within about 0.6 sec, with the residual motion persisting throughout.

4.2 Lowpass filtered torque input

To study the performance of the system with a lowpass Butterworth filter design a lowpass filtered bang-bang torque input was used and the system response was measured at the hub and end-point. A fourth-order lowpass Butterworth filter with a cutoff frequency at 10 Hz was designed and used for pre-processing the bang-bang torque input. Figure 5 shows the lowpass Butterworth filtered torque input. It is noted that the spectral energy input at the first and higher resonance frequencies of the system is reduced significantly with the lowpass Butterworth filtered torque input in comparison to that with the bang-bang torque input. The corresponding manipulator displacement at the hub is shown in Figure 6. It is noted that the desired steady-state level of response has reached within a similar time-scale as with the bang-bang torque input. However, oscillations in the response of the system have significantly been reduced, specially at the second and higher modes. The reduction in the level of oscillations at the first, second and third modes are by 10, 50 and 76 dB, respectively, in comparison to the bang-bang torque input. A similar level of reduction at the resonance modes of the system are evidenced in the hub velocity, end-point acceleration and end-point residual motion, as shown in Figure 7.

To study the performance of the system with a lowpass elliptic filter design a lowpass filtered bang-bang torque input was used and the system response was measured at the hub and end-point. Thus, with similar design specifications as the lowpass Butterworth filter, a third-order lowpass elliptic filter with a cutoff frequency at 10 Hz, stopband ripple of 30 dB and passband ripple of 3 dB was designed and used for pre-processing the bang-bang torque input. Figure 8 shows the lowpass elliptic filtered torque input. It is noted that the

spectral energy input at the first and higher resonance frequencies of the system is reduced to a similar level as with the lowpass Butterworth filtered torque input. The corresponding manipulator displacement at the hub is shown in Figure 9. It is noted that the desired steady-state level of response is reached within a similar time-scale as with the lowpass Butterworth filtered and bang-bang torque inputs. Oscillations in the response of the system have further been reduced at the first mode at the expense of slightly less reduction at the second and third mode in comparison to those with the lowpass Butterworth filtered torque input. The reduction in the level of oscillations at the first, second and third modes are by 12, 30 and 36 dB, respectively, with the lowpass elliptic filtered torque input in comparison to the bang-bang torque input. A similar level of reduction at the resonance modes of the system are evidenced in the hub velocity, end-point acceleration and end-point residual motion, as shown in Figure 10. In comparison to the lowpass Butterworth filtered torque input, it is noted that the reduction in the level of oscillations at the first mode is better. This is achieved by the steep roll-off at the cutoff of the elliptic filter in comparison to the Butterworth filter. Although, the reduction in the level of oscillations at the second and third modes with the lowpass Butterworth filtered torque input is significantly more than that with the lowpass elliptic filtered torque input, the level of vibrations as seen in Figures 7(c) and 10(c) is lower with the lowpass elliptic filtered torque input. This is due to the slightly larger reduction at the first mode with the lowpass elliptic filtered torque input in comparison to the lowpass Butterworth filtered torque input. Note further that the order of the filter achieving similar design specifications is lower with the elliptic design in comparison to the Butterworth design.

4.3 Bandstop filtered torque input

To investigate the system performance with bandstop filtered torque inputs both Butterworth and elliptic designs are considered. A bandstop filtered bang-bang torque input is used and the response measured at the hub and end-point. A requirement specification on studying the effect of attenuating the first mode, the first two modes and finally the first

three modes was set up.

To study the performance of the system with bandstop Butterworth filtered torque inputs, three fourth-order filters with a bandwidth of 5 Hz and centre frequencies at 12, 38 and 74 Hz respectively were designed and used to process the bang-bang torque input to the system. Figure 11 shows the bandstop Butterworth filtered torque inputs generated and utilised. It is noted that the spectral attenuation in the input in comparison to the bang-bang torque input in Figure 2, is by 30, 20 and 4 dB in the first, second and third modes respectively. The hub displacement, corresponding to each input in Figure 11, is shown in Figure 12 with the corresponding hub velocity, end-point acceleration and end-point residual motion in Figures 13, 14 and 15. It is noted in Figure 12 that the reduction in the response level at the first mode with the (first mode) bandstop Butterworth filtered torque input is by 38 dB in comparison to that with the bang-bang torque input. The reduction, additionally, at the second mode with the (first two modes) bandstop Butterworth filtered torque input is by 44 dB and, further, at the third mode with the (first three modes) bandstop Butterworth filtered torque input is by 32 dB. Such a level of reduction at the three resonance modes is also evidenced in the hub velocity, end-point acceleration and end-point residual motion, as shown in Figures 13, 14 and 15. Note that, although, significant reduction in the residual motion of the system is achieved with only a single (first mode) bandstop Butterworth filter, oscillations in the system response, due to the second and higher modes, are still noticeable. With two (first two modes) bandstop Butterworth filters the residual motion of the system has reduced to an acceptable level and further to a negligible level with three (first three modes) bandstop Butterworth filters. The speed of response, as noted, is of the same order as with the bang-bang torque input.

To study the performance of the system with bandstop elliptic filtered torque inputs, three third-order filters on the basis of the same specification requirements as the corresponding Butterworth filters above were designed, with a bandwidth of 5 Hz, stopband ripple of 20 dB, passband ripple of 1 dB and centre frequencies at 12, 38 and 74 Hz respectively. The filters were used to process the bang-bang torque input to the system. Figure 16 shows the bandstop elliptic filtered torque inputs generated and utilised. It is

noted that the spectral attenuation in the input in comparison to the bang-bang torque input in Figure 2, is by 12, 12 and 4 dB in the first, second and third modes respectively. The hub displacement, corresponding to each input in Figure 16, is shown in Figure 17 with the corresponding hub velocity, end-point acceletation and end-point residual motion in Figures 18, 19 and 20. It is noted in Figure 17 that the reduction in the response level at the first mode with the (first mode) bandstop elliptic filtered torque input is by 34 dB in comparison to that with the bang-bang torque input. The reduction, additionally, at the second mode with the (first two modes) bandstop elliptic filtered torque input is by 24 dB and, further, at the third mode with the (first three modes) bandstop Butterworth filtered torque input is by 18 dB. Such a level of reduction at the three resonance modes is also evidenced in the hub velocity, end-point acceletation and end-point residual motion, as shown in Figures 18, 19 and 20. Note that, although, significant reduction in the residual motion of the system is achieved with only a single (first mode) bandstop elliptic filter, oscillations in the system response, due to the second and higher modes, are still noticeable. With two (first two modes) bandstop elliptic filters the residual motion of the system has reduced to an acceptable level and further to a negligible level with three (first three modes) bandstop elliptic filters. The speed of response, as noted, is of the same order as with the bang-bang torque input. It is further noted that the speed of response as well as reduction in the level of residual motion of the system with the elliptic bandstop filtered torque inputs are very close to those with the Butterworth bandstop filtered torque inputs. The difference in the two cases is negligibly small.

Comparing the results achieved with the bandstop and lowpass filtered torque inputs reveals that better performance at reduction of level of residual motion (vibration) of the system is achieved with lowpass filtered torque inputs. This is due to the indiscriminate spectral attenuation in the lowpass filtered torque input at all the resonance modes of the system. Utilisation of bandstop filters, however, is advantageous in that spectral attenuation in the input at selected resonance modes of the system can be achieved. Thus, the open-loop control strategy based on bandstop filters is optimum in this sense. Note that this

strategy can also be viewed as equivalent to designing a controller with zeros that cancel out the system poles (resonance modes).

5 Conclusion

The development of open-loop control strategies for flexible manipulator systems using filtered torque inputs has been presented and verified within a constrained planar single-link flexible manipulator environment. Open-loop control methods involve the development of the control input by considering the physical and vibrational properties of the flexible manipulator system. The control input is to minimise the energy input at system resonance modes so that system vibrations are reduced. Lowpass and bandstop filtered torque input functions have been developed and investigated in an open-loop control configuration. Remarkable improvement in the reduction of system vibrations has been achieved with these control functions as compared to a bang-bang torque input. Bandstop filters can be utilised to reduce spectral energy at selected (dominant) resonance modes of the system. However, if the spectral energy around a large number of resonance modes of the system contribute significantly to system vibrations, it will be more desirable to utilise lowpass filtered command inputs.

6 References

ALBERTS, T. E., LOVE, L. J., BAYO, E. and MOULIN, H. (1990). Experiments with end-point control of a flexible link using the inverse dynamics approach and passive damping, *Proceedings of American Control Conference*, San diego, May, **1**, pp. 350-355.

ASPINWALL, D. M. (1980). Acceleration profiles for minimizing residual response, *ASME Journal of Dynamic Systems, Measurement and Control*, **102**, (1), pp. 3-6.

BANKS, S. P. (1990). *Signal processing, image processing and pattern recognition.* Prentice-Hall, London.

BAYO, E. (1988). Computed torque for the position control of open-loop flexible robots, *Proceeding of IEEE International Conference on Robotics and Automation*, Philadelphia, April, pp. 316-321.

DELLMAN, R., GLICKSBER, I. and GROSS, O. (1956). On the bang-bang control problem, *Quarterly of Applied Mechanics*, **14**, (1), pp. 11-18.

DWIGHT, H. B. (1957). *Tables and integrals and other mathematical data*, 3rd Edition, Macmillan, New York.

JACKSON, L. B. (1989). *Digital filters and signal processing*, Kluwer Academic Publishers, London.

JAYASURIYA, S. and CHOUPRA, S. (1991). On the finite settling time and residual vibration control of flexible structures, *Journal of Sound and Vibration*, **148**, (1), pp. 117-136.

MECKL, P. H. and SEERING, W. P. (1985a). Active damping in a three-axis robotic manipulator, *Journal of Vibration, Acoustics, Stress and Reliability in Design*, **107**, (1), pp. 38-46.

MECKL, P. H. and SEERING, W. P. (1985b). Minimizing residual vibration for point-to-point motion, *Journal of Vibration, Acoustics, Stress and Reliability in Design*, **107**, (4), pp. 378-382.

MECKL, P. H. and SEERING, W. P. (1987). Reducing residual vibration in systems with time-varying resonances, *Proceedings of IEEE International Conference on Robotics and Automation*, Rayleigh, March, pp. 1690-1695.

MECKL, P. H. and SEERING, W. P. (1988). Controlling velocity limited system to reduce residual vibration, *Proceeding of IEEE International Conference on Robotics and Automation*, Philadelphia, April, pp. 1428-1433.

MECKL, P. H. and SEERING, W. P. (1990). Experimental evaluation of shaped inputs to reduce vibration of a cartesian robot, *Transactions of the ASME Journal of Dynamic Systems, Measurement and Control*, **112**, (6), pp. 159-165.

MEIROVITCH, L. (1967). *Analytical methods in vibrations*, Macmillan New York.

MOULIN, H. and BAYO, E. (1991). On the accuracy of end-point trajectory tracking for flexible arms by noncausal inverse dynamic solution, *Transactions of the ASME Journal of Dynamic Systems, Measurement and Control*, **113**, (2), pp. 320-324.

ONSAY, T. and AKAY, A. (1991). Vibration reduction of a flexible arm by time optimal open-loop control, *Journal of Sound and Vibration*, **142**, (2), pp. 283-300.

SANGVERAPHUNSIRI, V. (1984). *The optimal control and design of a flexible manipulator*, PhD thesis, School of Mechanical Engineering, Georgia Institute of Technology, USA.

SINGER, N. C. and SEERING, W. P. (1988). Using causal shaping techniques to reduce residual vibration, *Proceedings of IEEE International Conference on Robotics and Automation*, Philadelphia, April, pp. 1434-1439.

SINGER, N. C. and SEERING, W. P. (1990). Preshaping command inputs to reduce systems vibration, *Transactions of the ASME Journal of Dynamic Systems, Measurement and Control*, **112**, (1), pp. 76-82.

SINGER, N. C. and SEERING, W. P. (1992). An extension of command shaping methods for controlling residual vibration using frequency sampling, *Proceedings of IEEE International Conference on Robotics and Automation*, Nice, May, pp. 800-805.

SWIGERT, J. C. (1980). Shaped torque techniques, *Journal of Guidance and Control*, **3**, (5), pp. 460-467.

THE MATHWORKS. (1992). *Simulink user's guide*, The Mathworks Inc, Massachussets.

TOKHI, M. O., POERWANTO, H. and AZAD, A. K. M. (1995). *Dynamic simulation of flexible manipulator systems with structural damping*, Research Report No. 595, Department of Automatic Control and Systems Engineering, The University of Sheffield, UK.

WANG, S. (1986). Open-loop control of a flexible robot manipulator, *International Journal of Robotics and Automation*, **1**, (2), pp. 54-57.

ZVEREV, A. I. (1967). *Handbook of filter synthesis*, Wiley, New York.

Table 1: Physical dimensions and characteristics of the flexible manipulator.	
Length	960 mm
Thickness	3.2004 mm
Width	19.008 mm
Mass density per volume	2710 kgm^{-3}
Young Modulus	7.11×10^{10} Nm^{-2}
Area moment of inertia	5.1924×10^{-11} m^4
Hub inertia	5.86×10^{-4} kgm^2
Manipulator moment of inertia	0.04862 kgm^2
First resonance mode	12.137 Hz
Second resonance mode	36.132 Hz
Third resonance mode	88.86 Hz

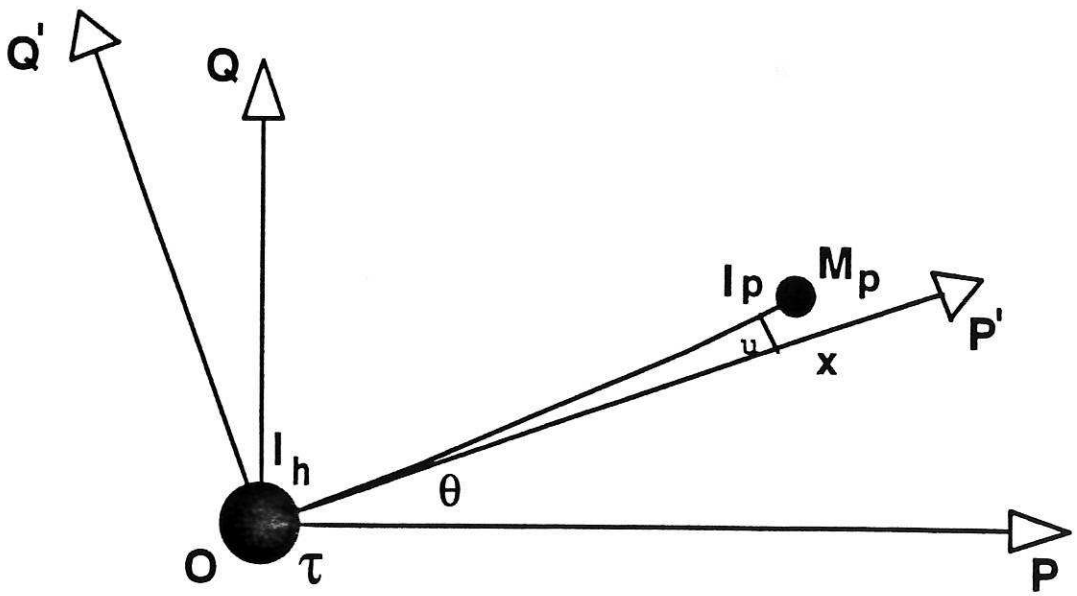

Figure 1: Description of the flexible manipulator system.

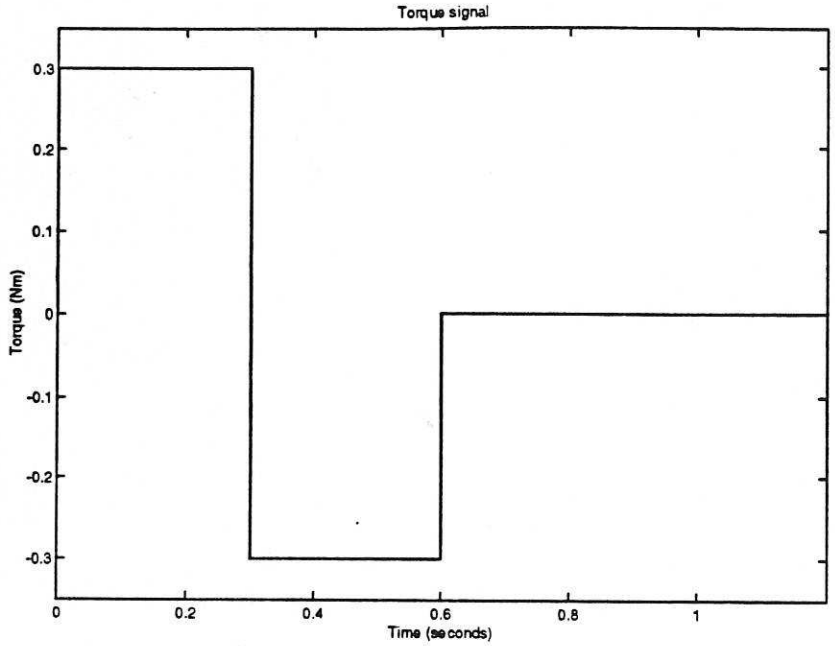

(a)

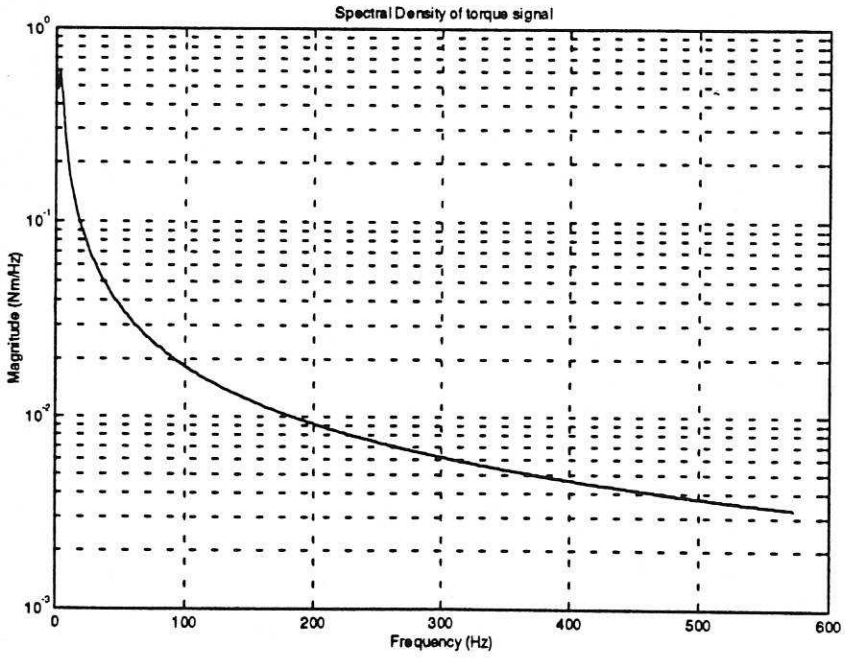

(b)

Figure 2: The bang-bang torque input;
(a) Time-domain.
(b) Spectral density.

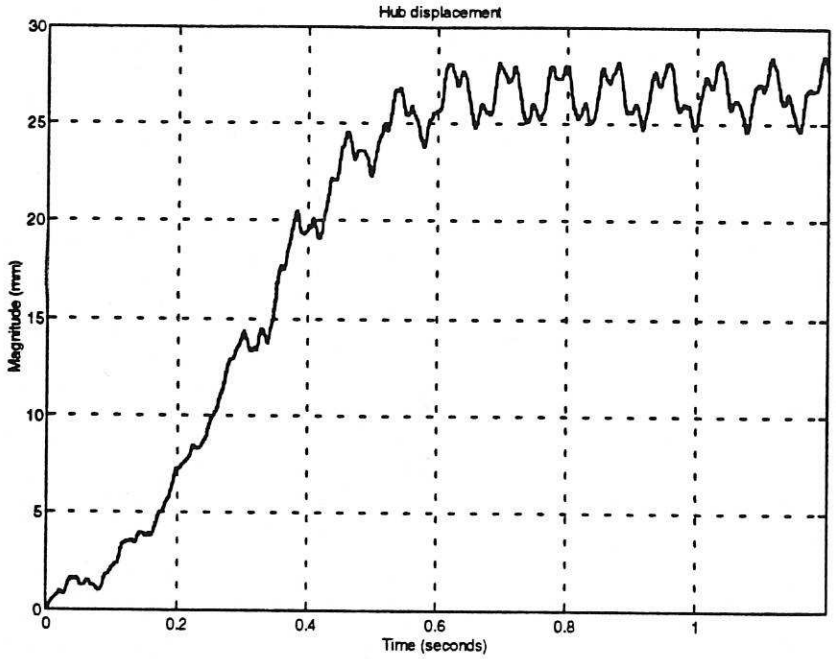

(a)

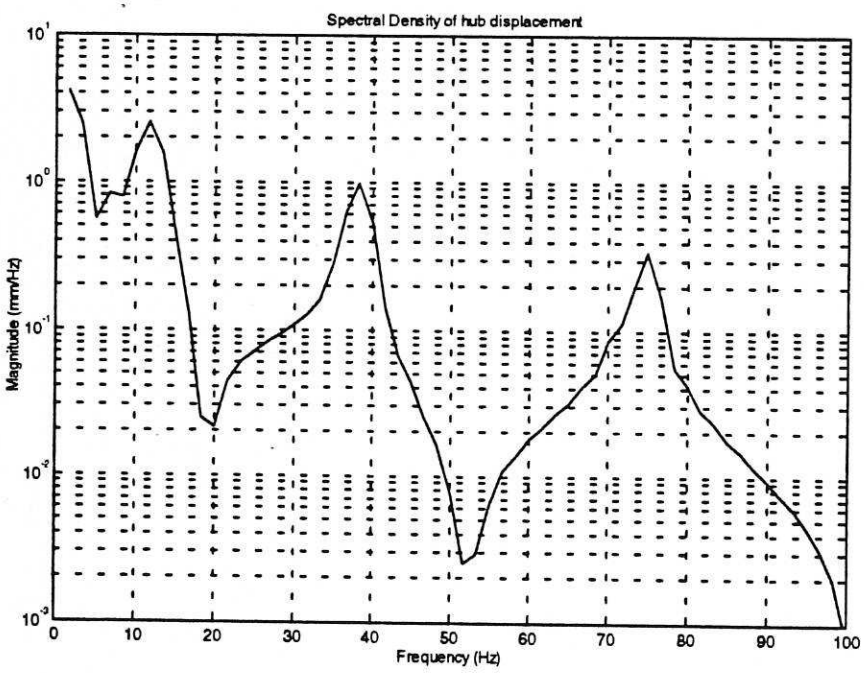

(b)

Figure 3: Hub displacement with the bang-bang torque input;
(a) Time-domain.
(b) Spectral density.

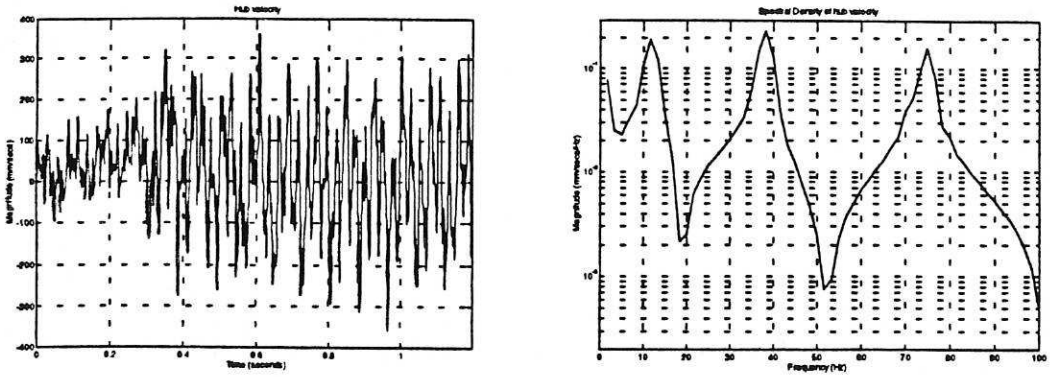

(a)

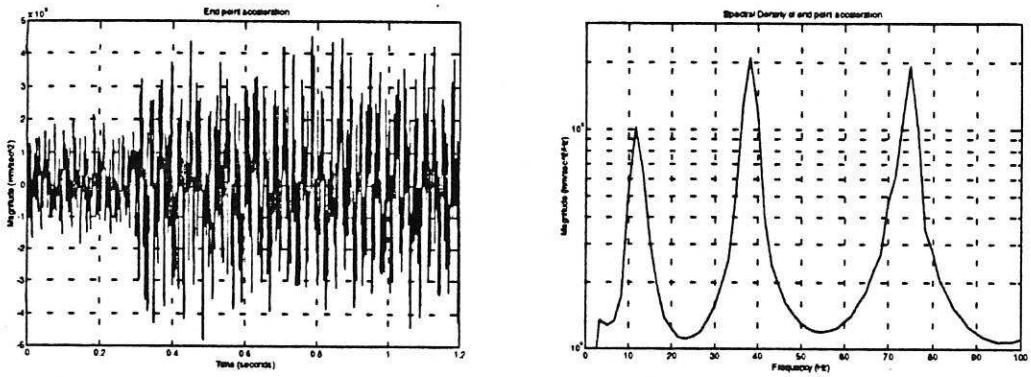

(b)

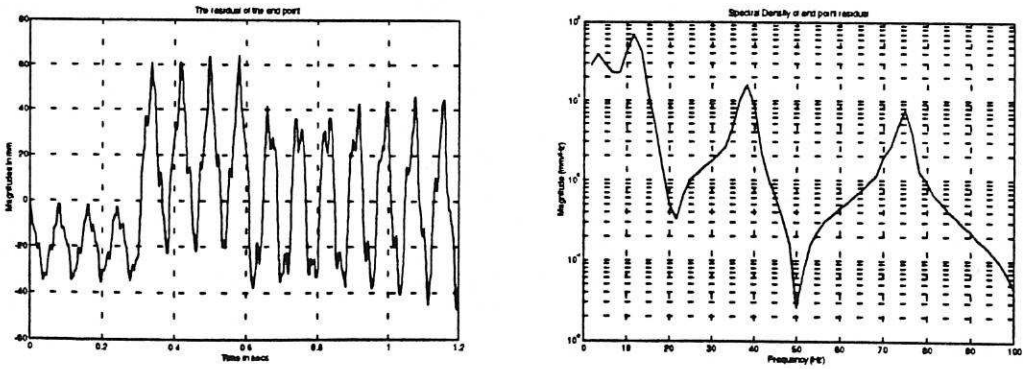

(c)

Figure 4: System response with the bang-bang torque input;
(a) Hub velocity.
(b) End-point acceleration.
(c) End-point residual motion.

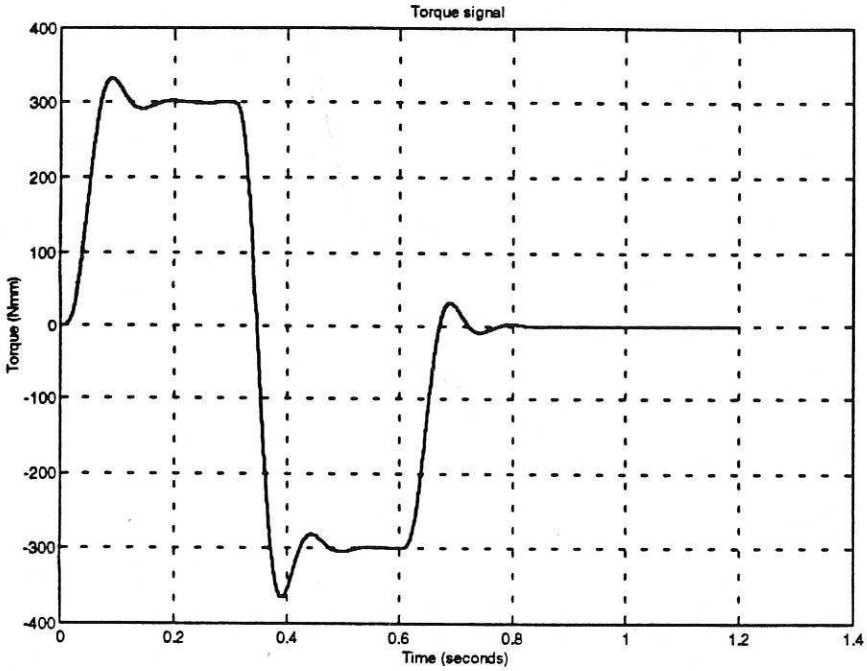

(a)

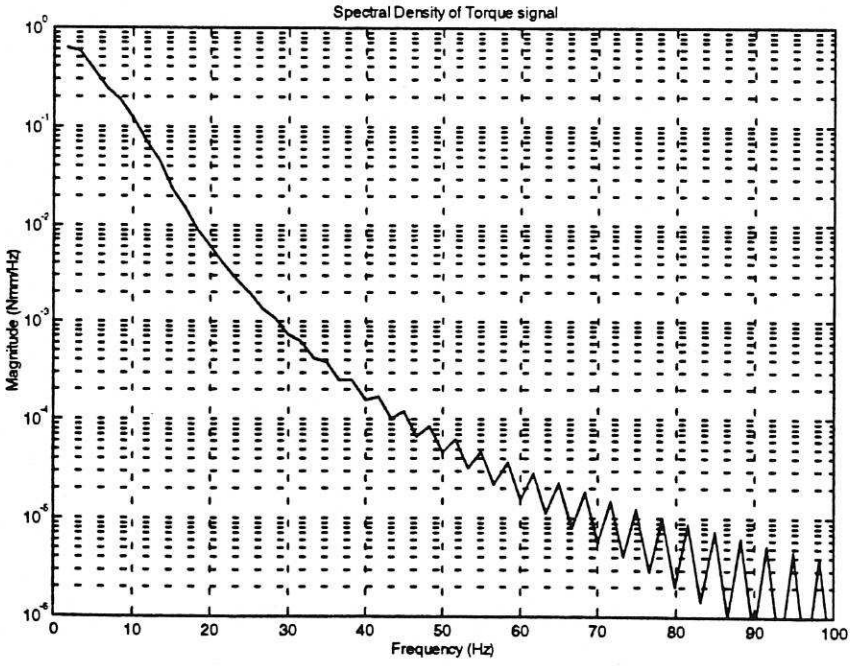

(b)

Figure 5: Lowpass Butterworth filtered torque input;
(a) Time-domain.
(b) Spectral density.

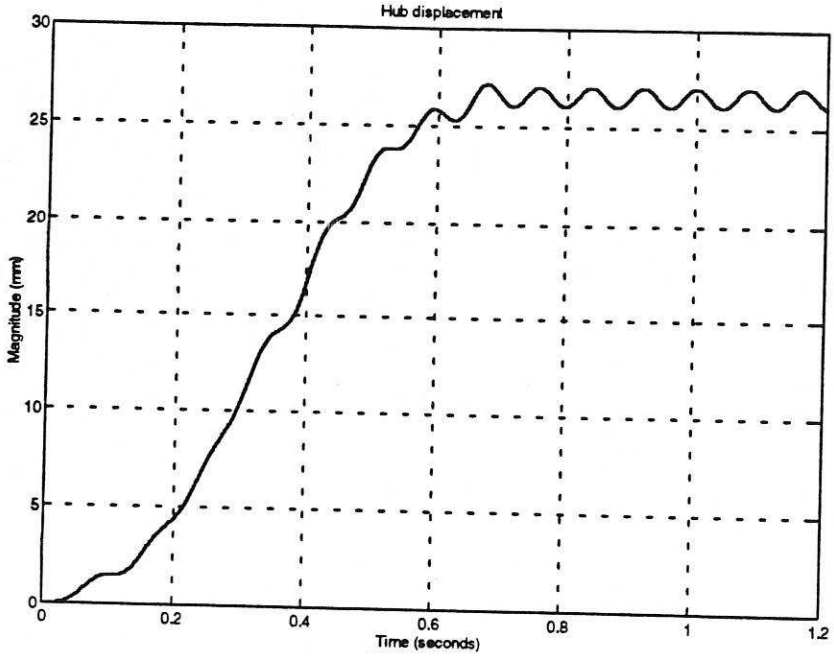

(a)

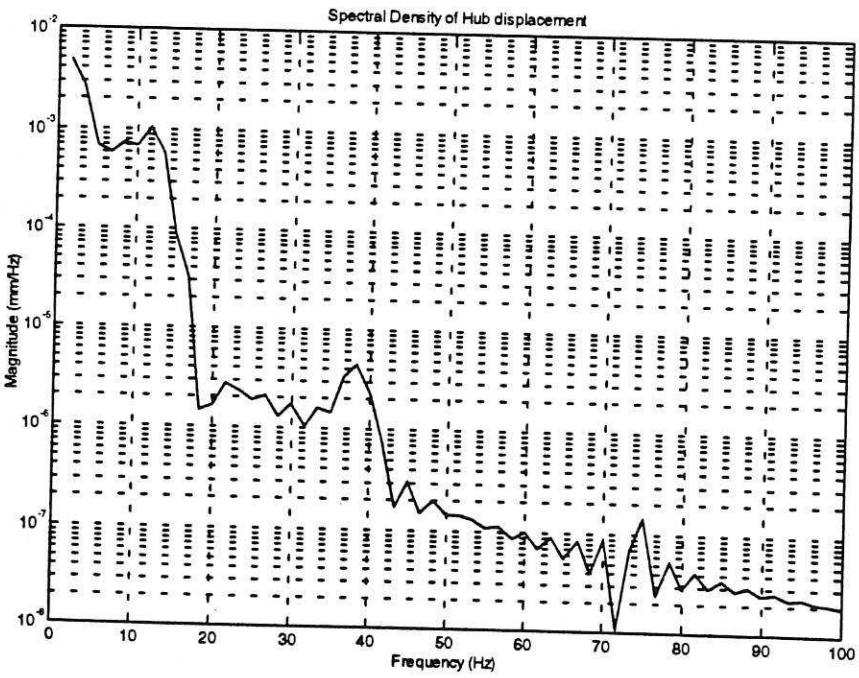

(b)

Figure 6: Hub displacement with the lowpass Buttterworth filtered torque input;
(a) Time-domain.
(b) Spectral density.

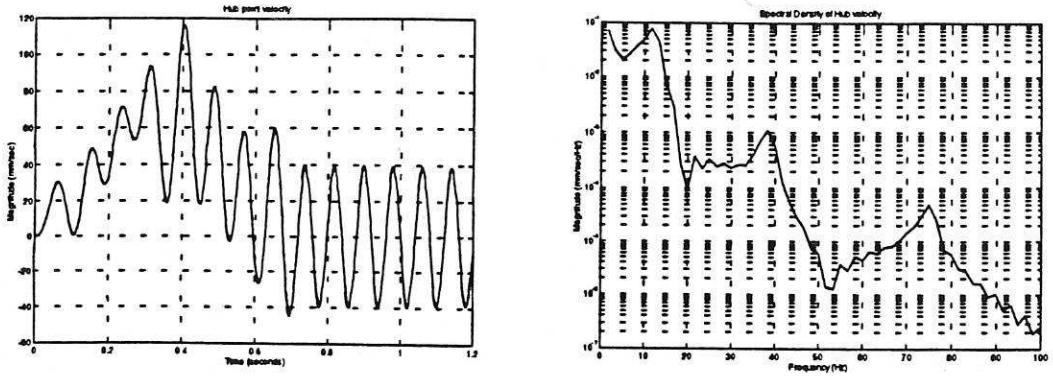

(a)

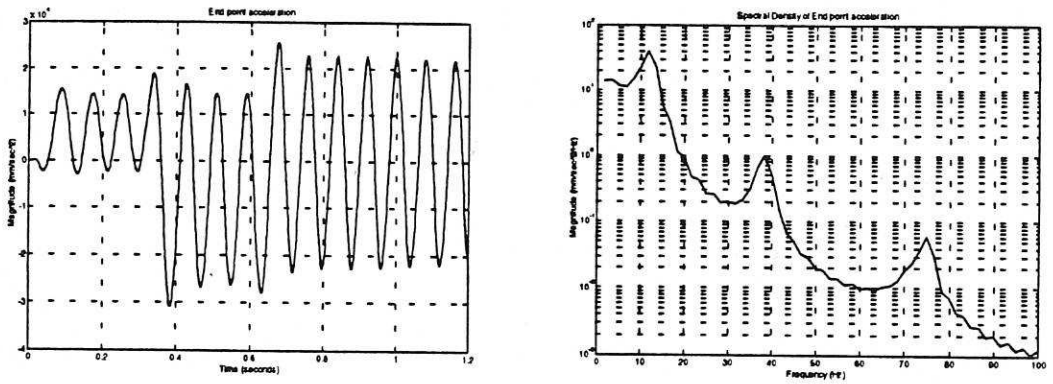

(b)

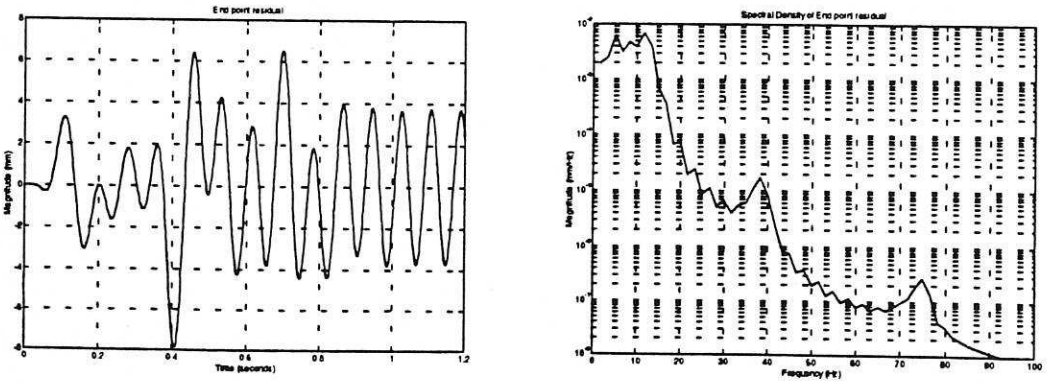

(c)

Figure 7: System response with the lowpass Buttterworth filtered torque input;
(a) Hub velocity.
(b) End-point acceleration.
(c) End-point residual motion.

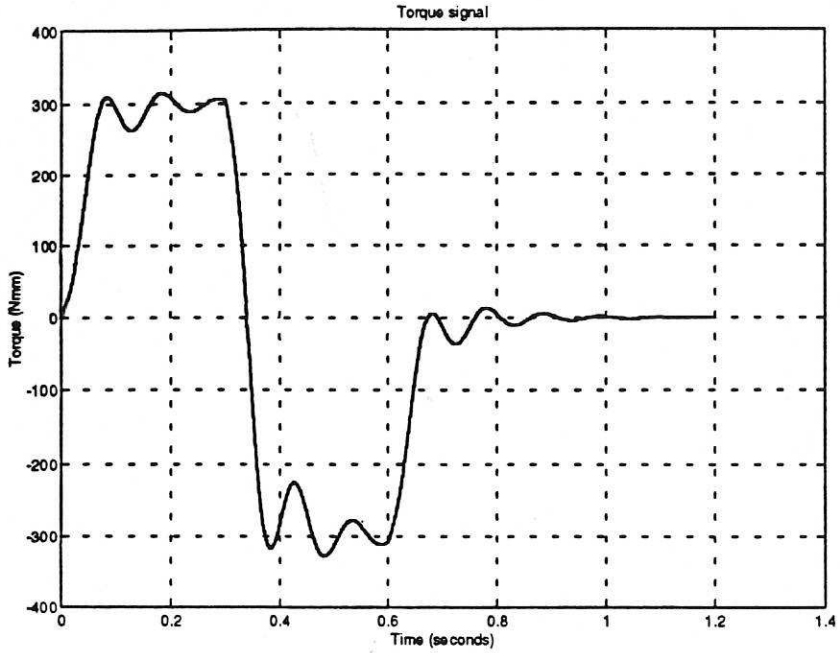

(a)

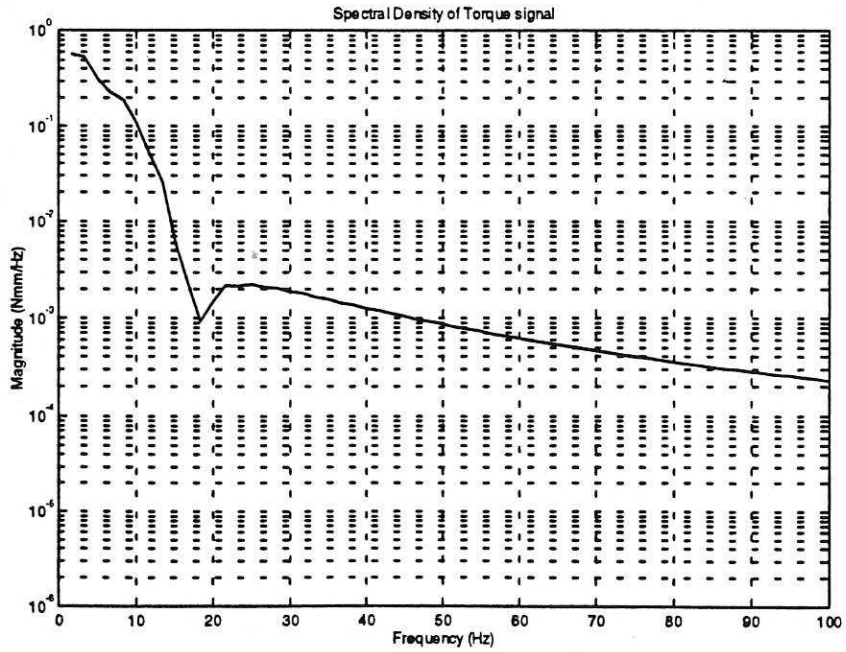

(b)

Figure 8: Lowpass elliptic filtered torque input;
(a) Time-domain.
(b) Spectral density.

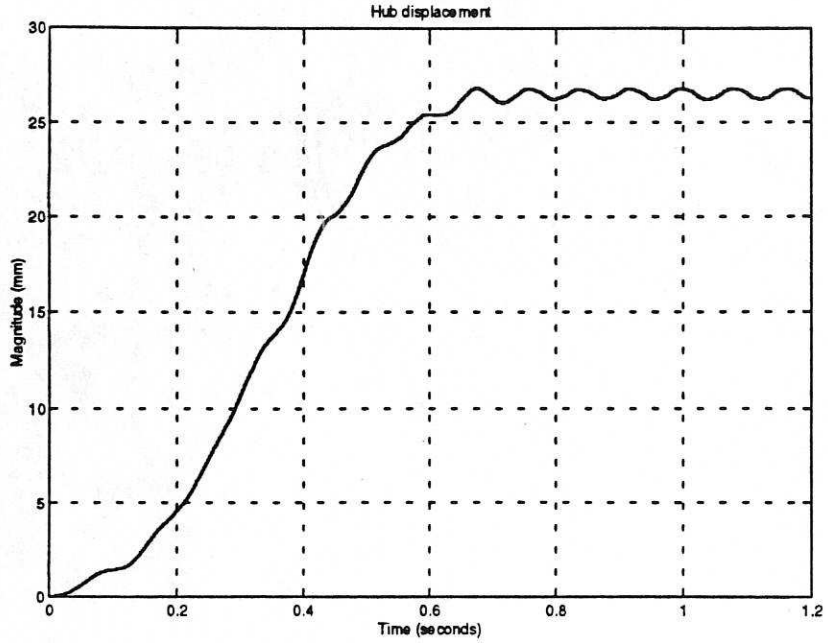

(a)

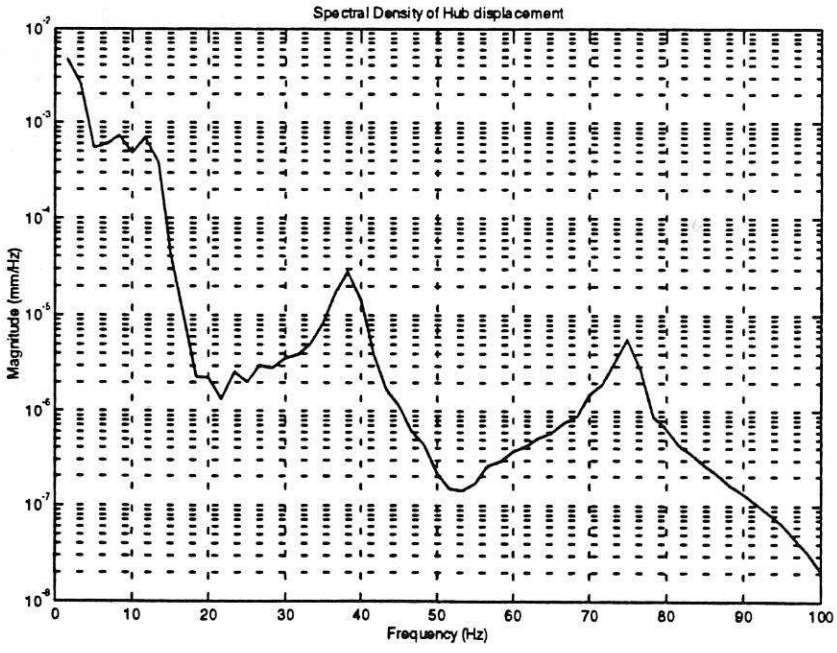

(b)

Figure 9: Hub displacement with the lowpass elliptic filtered torque input;
(a) Time-domain.
(b) Spectral density.

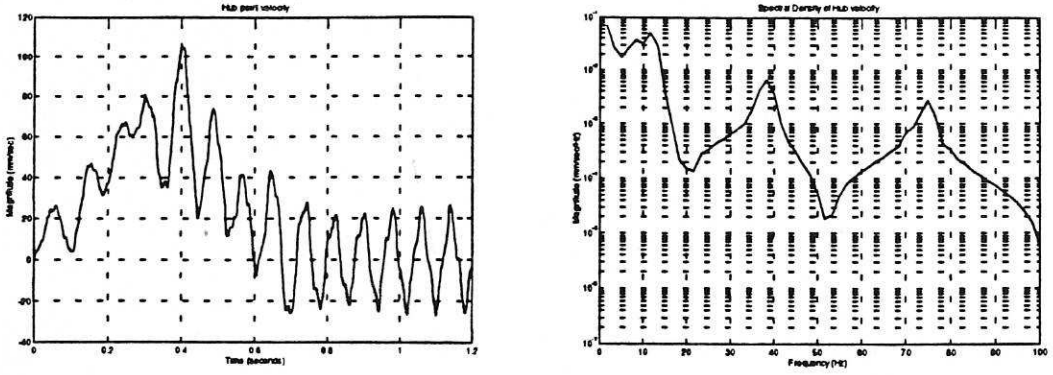

(a)

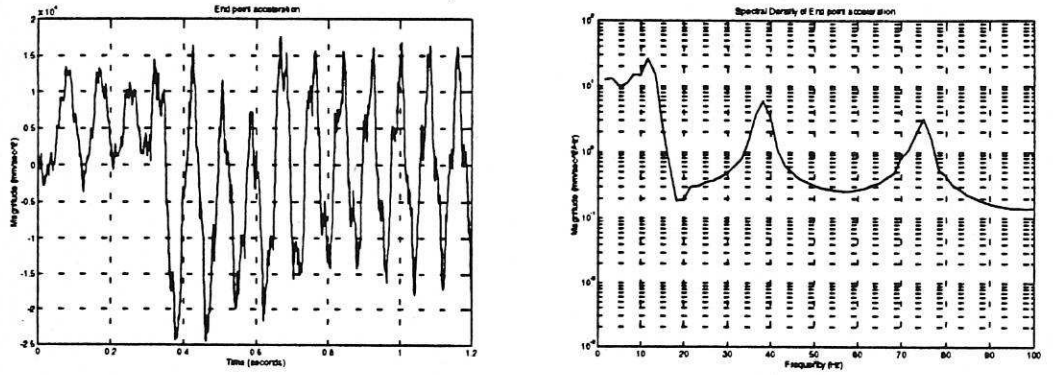

(b)

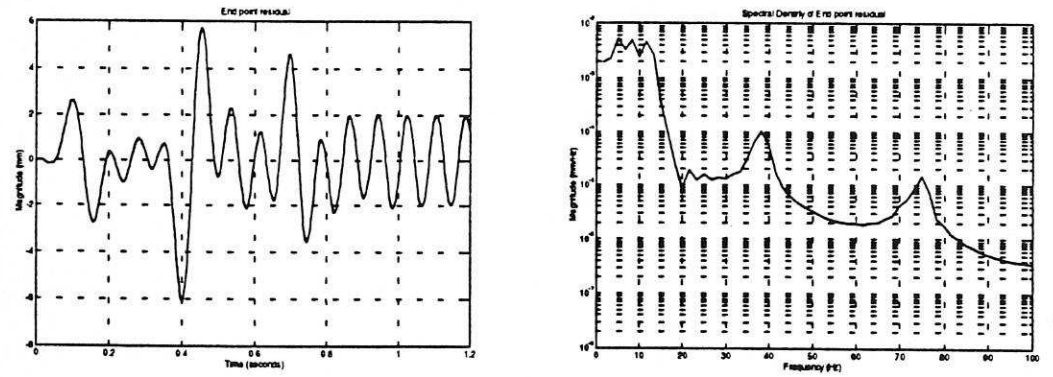

(c)

Figure 10: System response with the lowpass elliptic filtered torque input;
(a) Hub velocity.
(b) End-point acceleration.
(c) End-point residual motion.

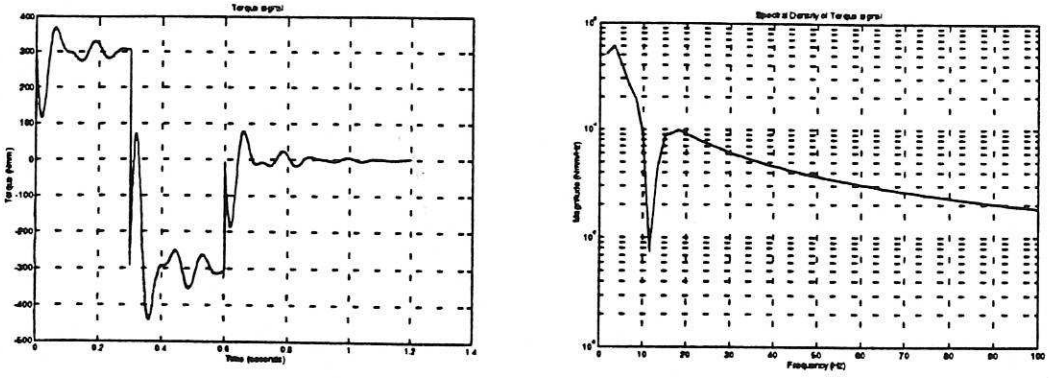

(a)

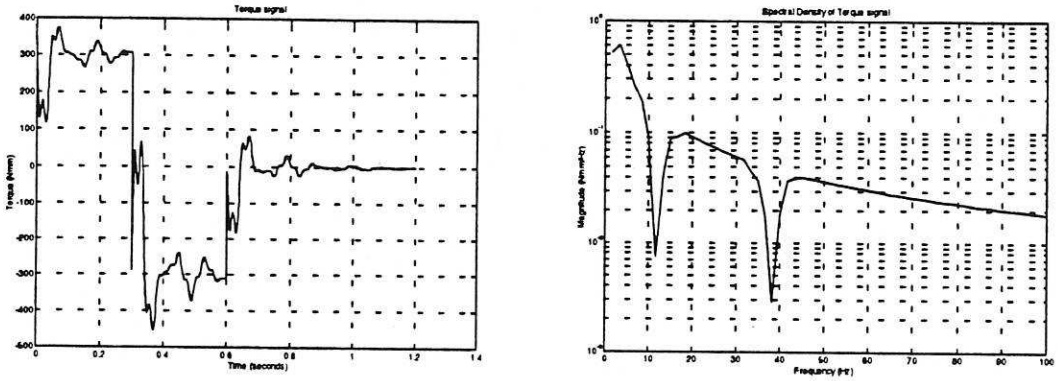

(b)

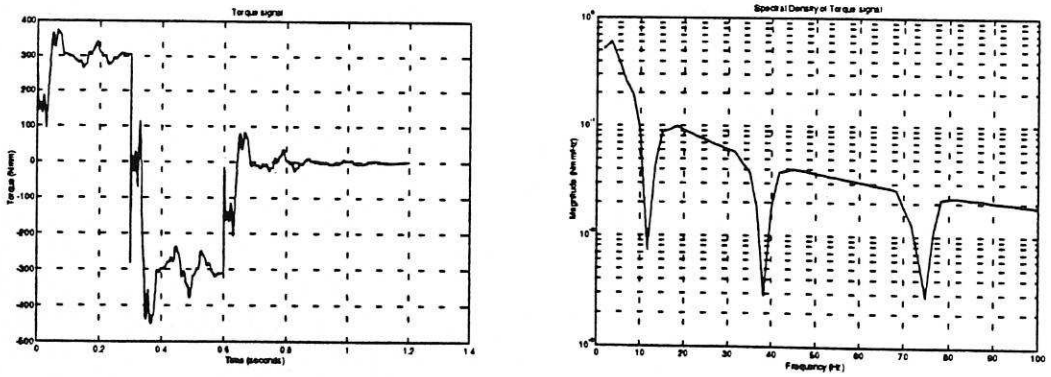

(c)

Figure 11: Bandstop Butterworth filtered torque input;
(a) First mode.
(b) The first two modes.
(c) The first three modes.

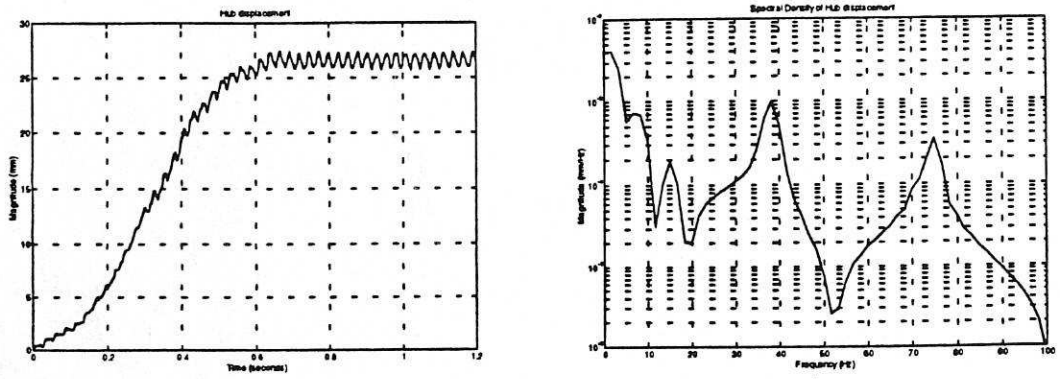

(a)

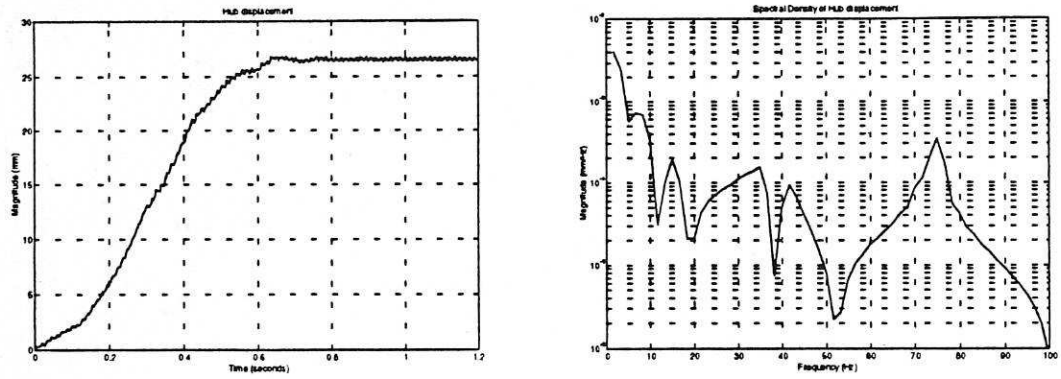

(b)

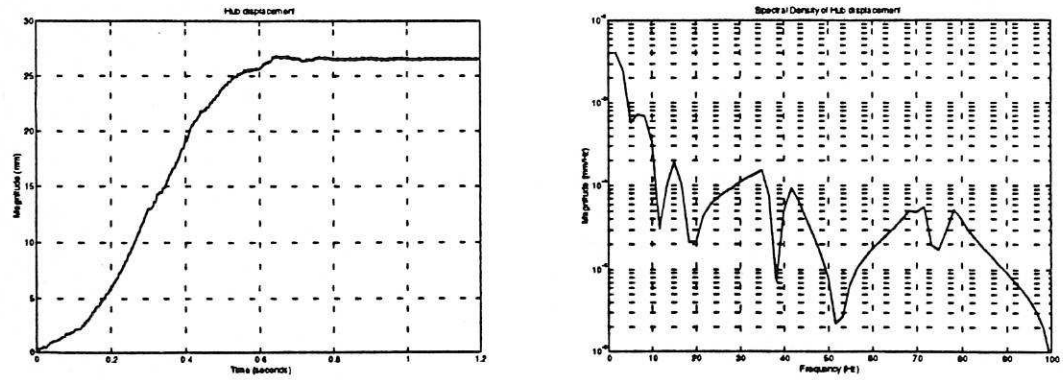

(c)

Figure 12: Hub displacement with bandstop Butterworth filtered torque input;
(a) First mode.
(b) The first two modes.
(c) The first three modes.

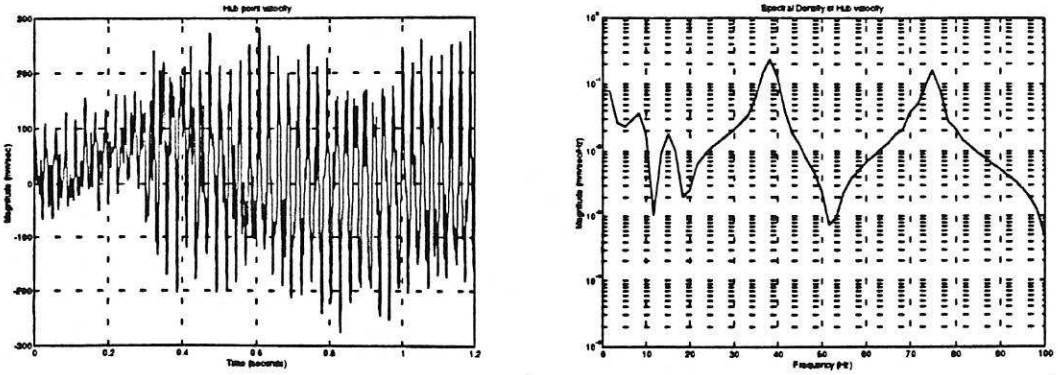

(a)

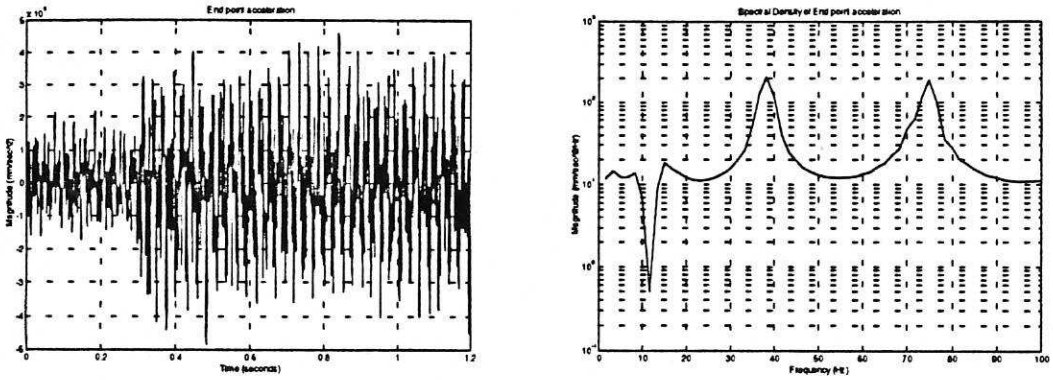

(b)

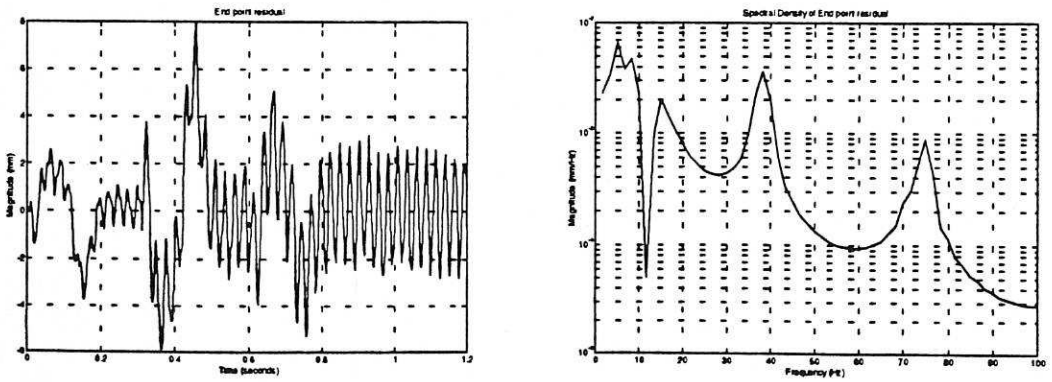

(c)

Figure 13: System response with the (first mode) bandstop Butterworth filtered torque input;
(a) Hub velocity.
(b) End-point acceleration.
(c) End-point residual motion.

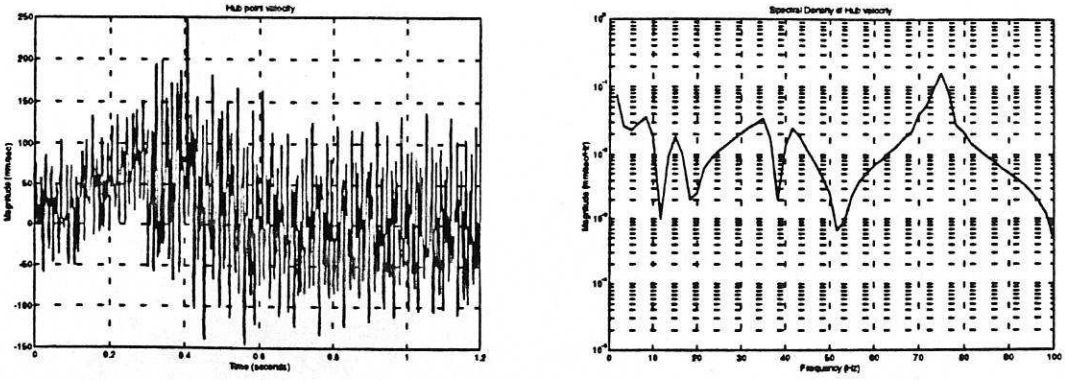

(a)

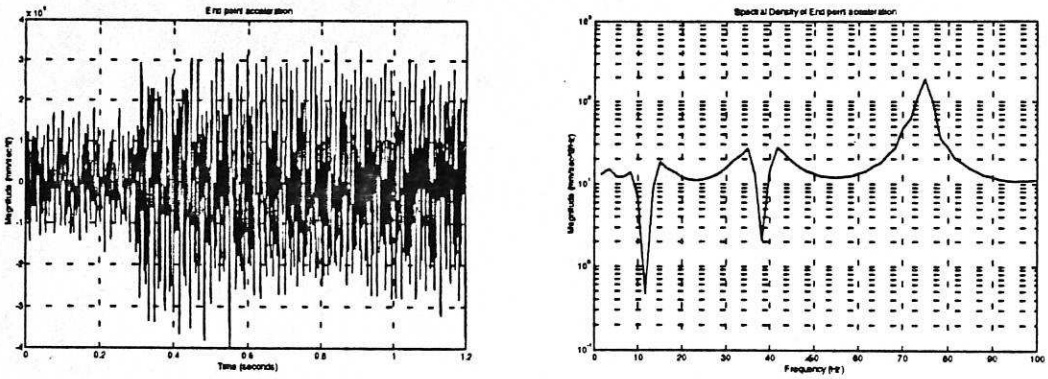

(b)

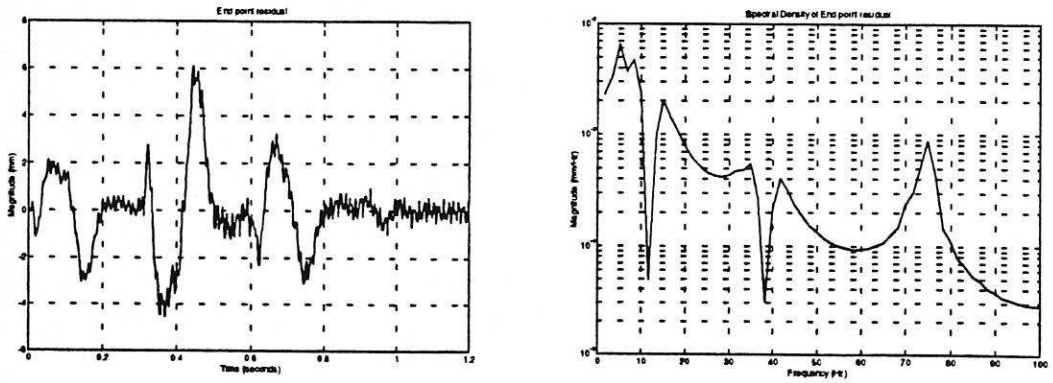

(c)

Figure 14: System response with the (first two modes) bandstop Butterworth filtered torque input;
(a) Hub velocity.
(b) End-point acceleration.
(c) End-point residual motion.

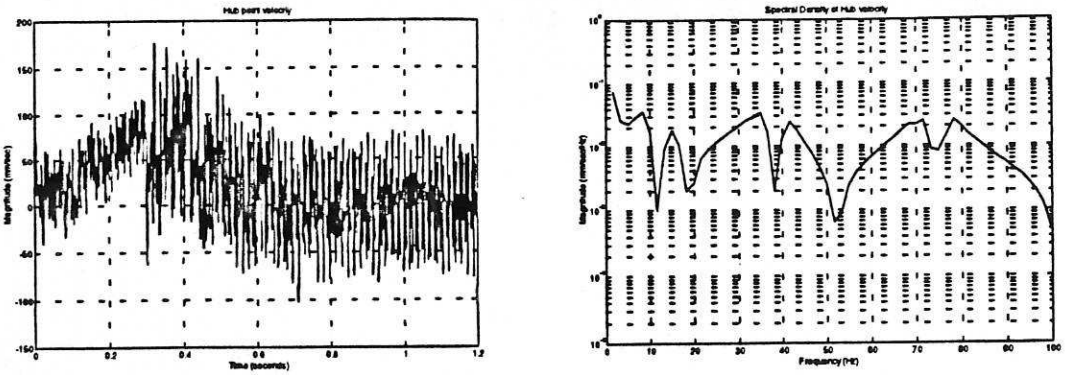

(a)

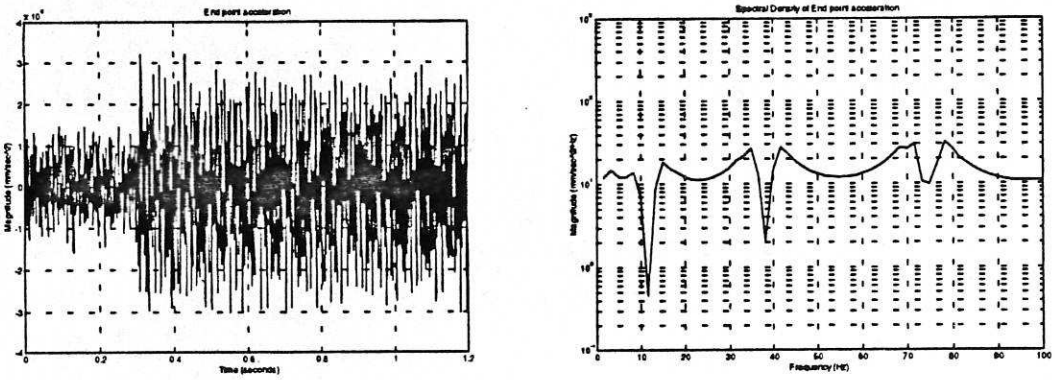

(b)

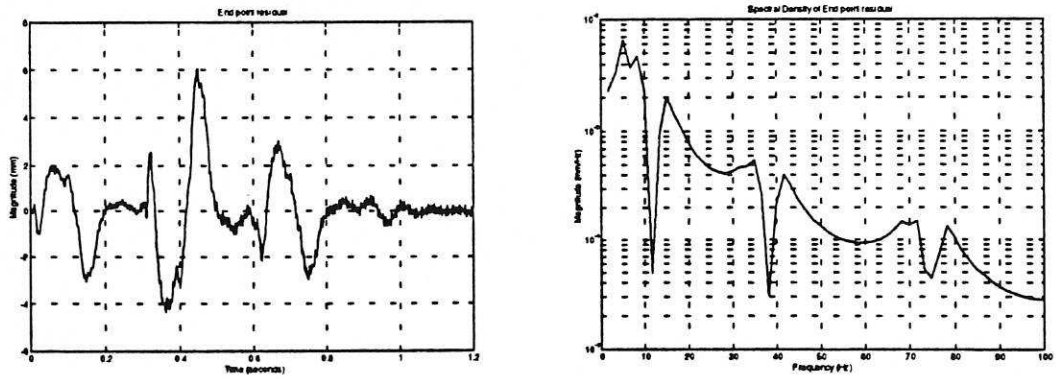

(c)

Figure 15: System response with the (first three modes) bandstop Butterworth filtered torque input;
(a) Hub velocity.
(b) End-point acceleration.
(c) End-point residual motion.

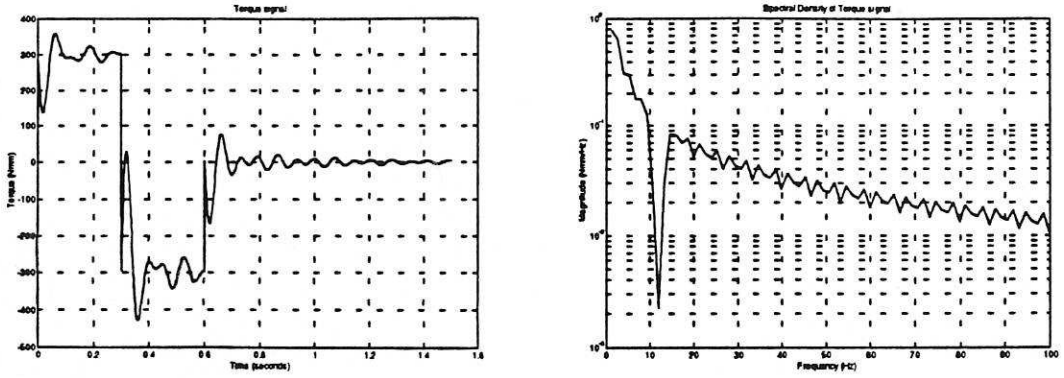

(a)

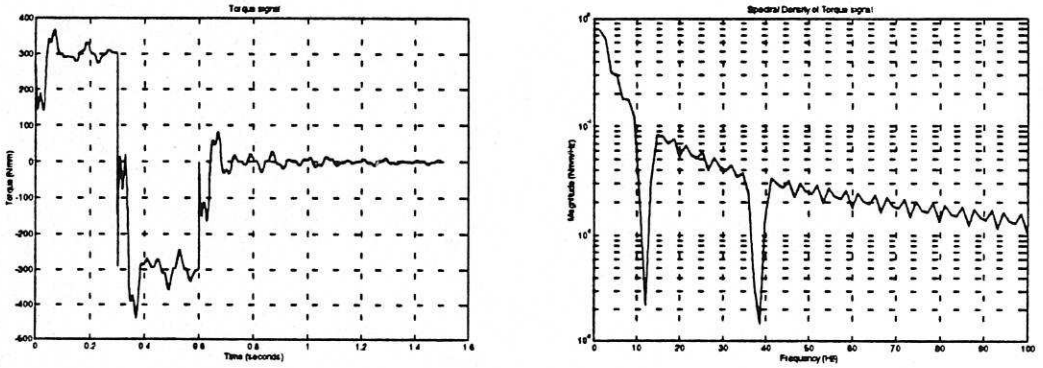

(b)

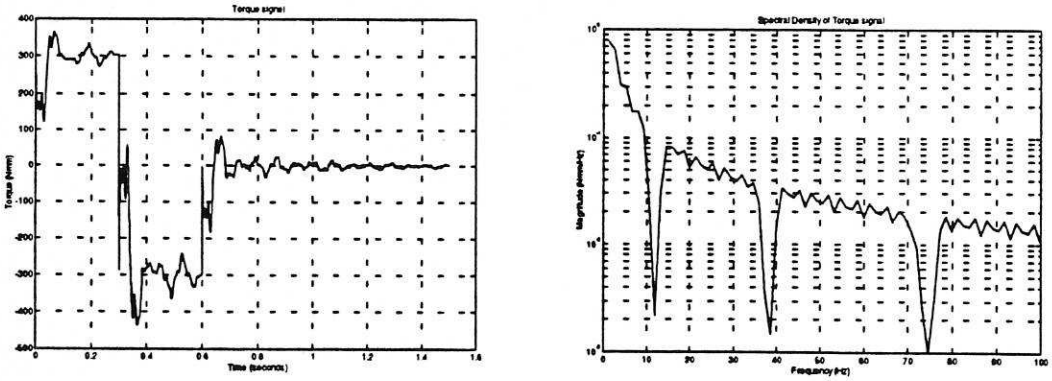

(c)

Figure 16: Bandstop elliptic filtered torque input;
(a) First mode.
(b) The first two modes.
(c) The first three modes.

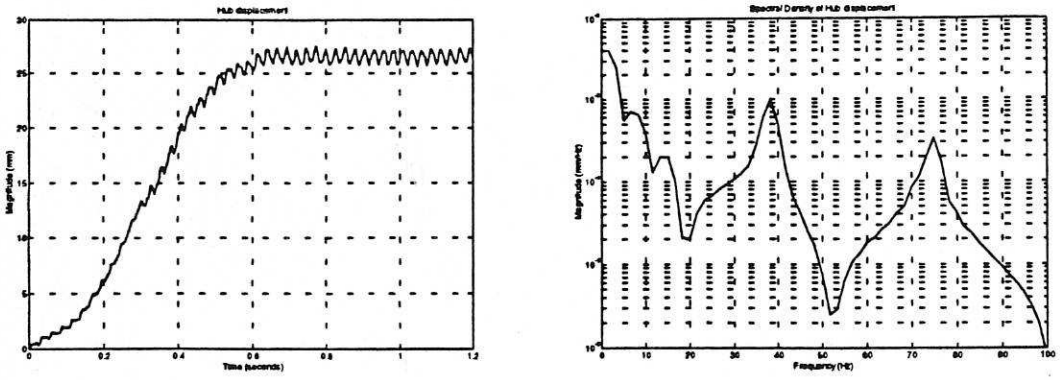

(a)

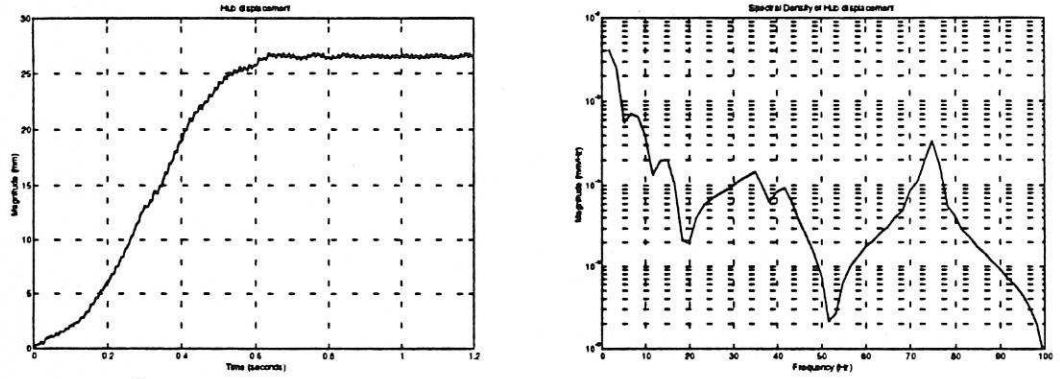

(b)

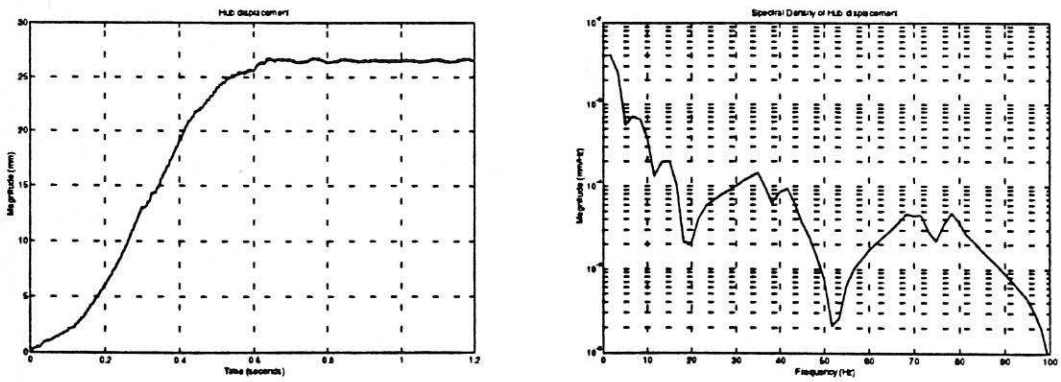

(c)

Figure 17: Hub displacement with bandstop elliptic filtered torque input;
(a) First mode.
(b) The first two modes.
(c) The first three modes.

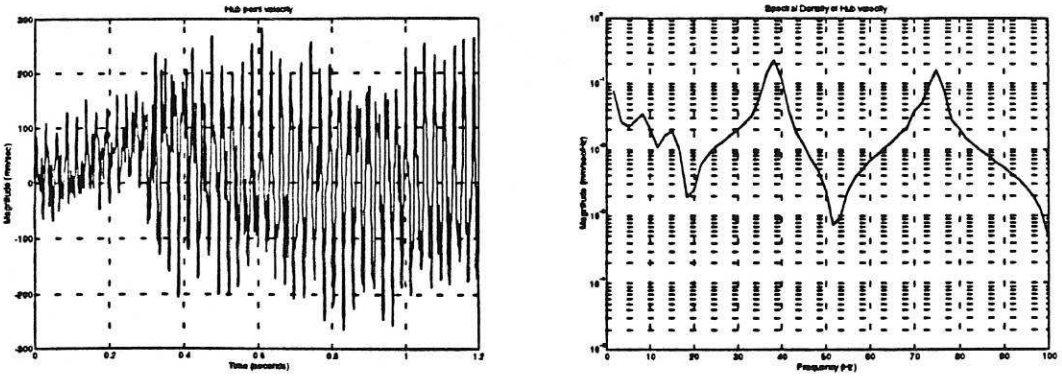

(a)

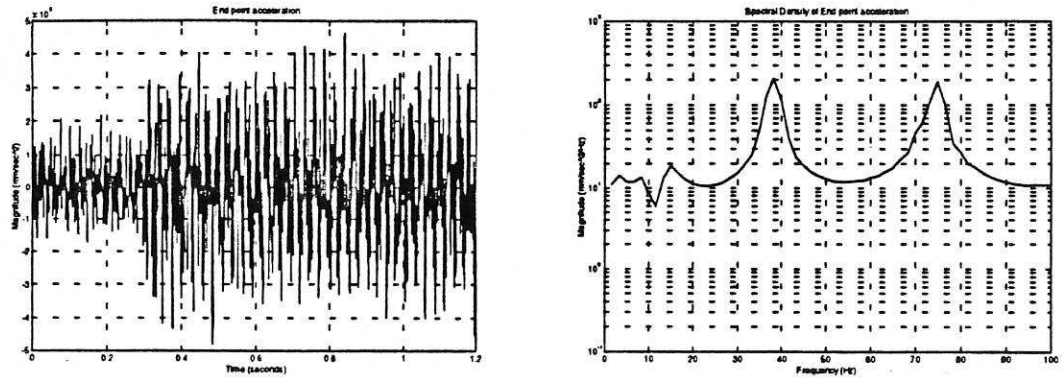

(b)

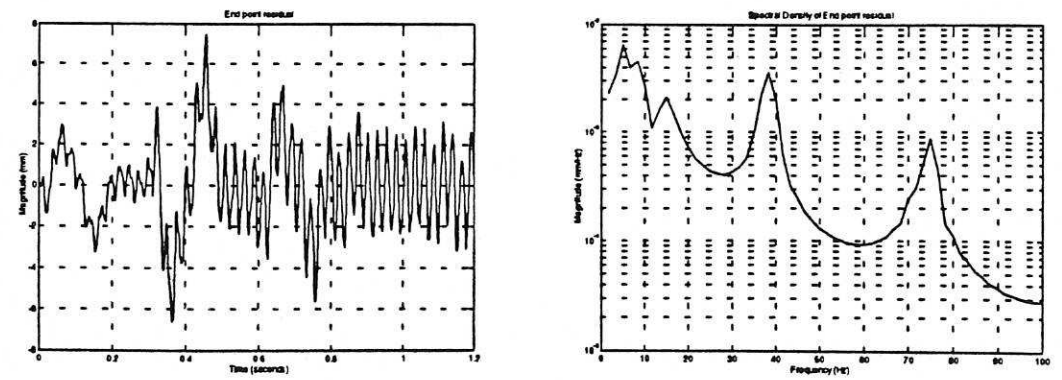

(c)

Figure 18: System response with the (first mode) bandstop elliptic filtered torque input;
(a) Hub velocity.
(b) End-point acceleration.
(c) End-point residual motion.

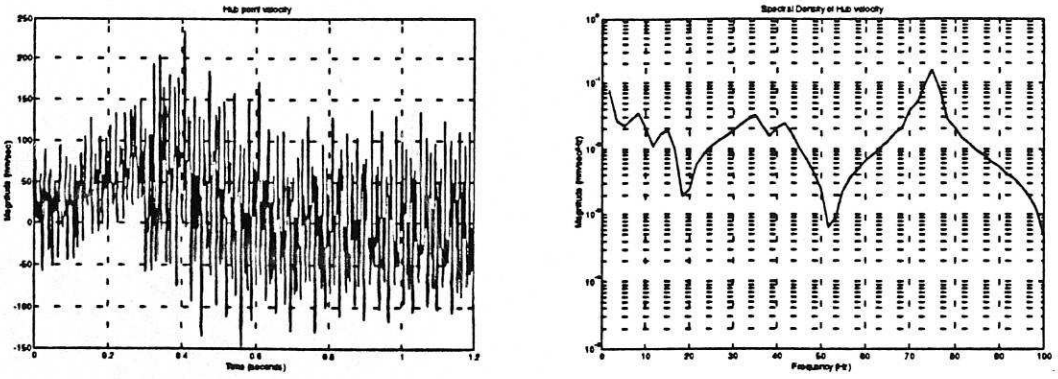

(a)

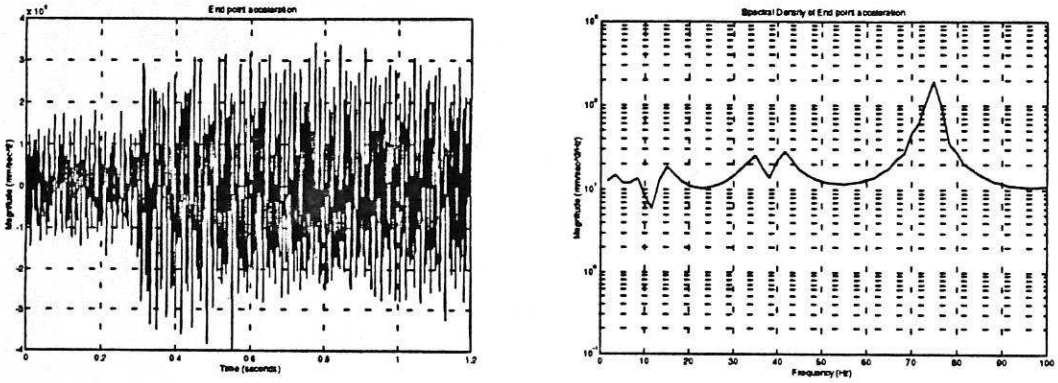

(b)

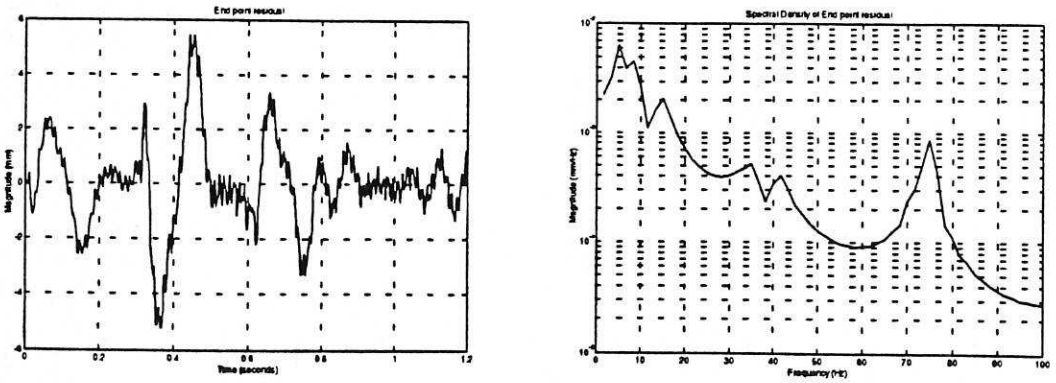

(c)

Figure 19: System response with the (first two modes) bandstop elliptic filtered torque input;
(a) Hub velocity.
(b) End-point acceleration.
(c) End-point residual motion.

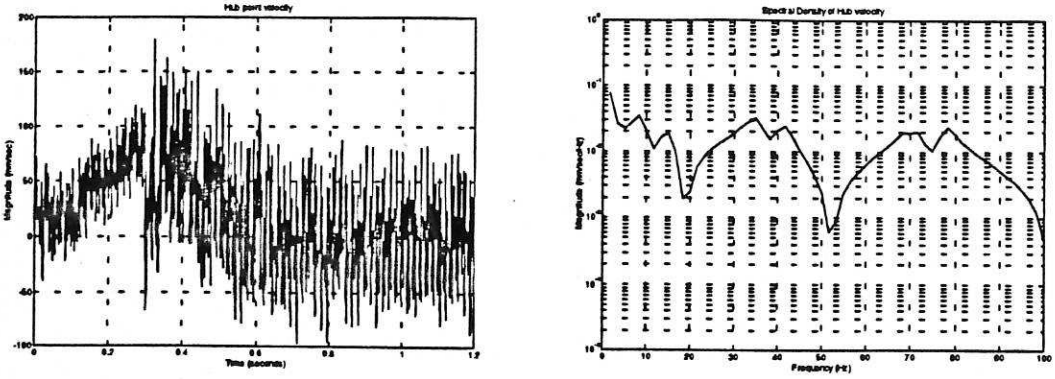

(a)

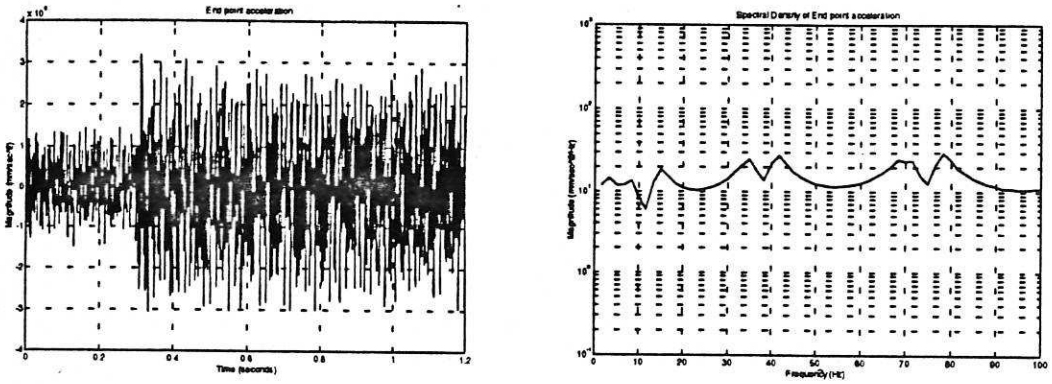

(b)

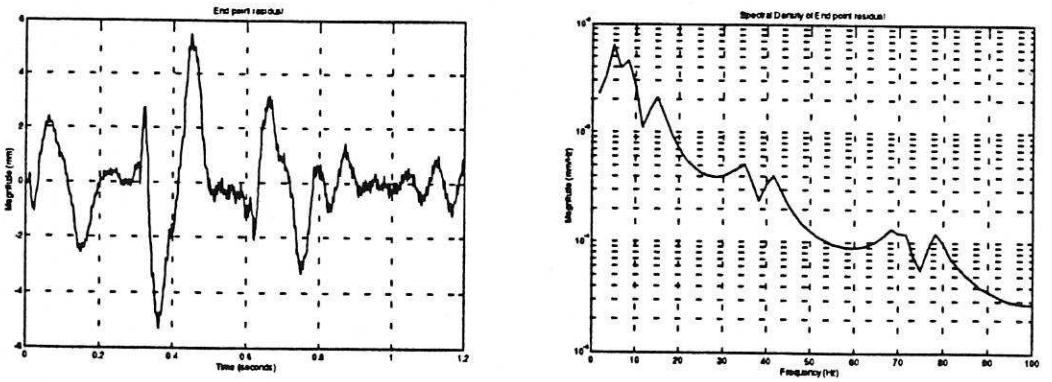

(c)

Figure 20: System response with the (first three modes) bandstop elliptic filtered torque input;
(a) Hub velocity.
(b) End-point acceleration.
(c) End-point residual motion.